

# VU Research Portal

## Regulation of neurotransmitter release by C-domain Ca<sup>2</sup>-sensors

Bourgeois-Jaarsma, Q.

2020

### **document version**

Publisher's PDF, also known as Version of record

[Link to publication in VU Research Portal](#)

### **citation for published version (APA)**

Bourgeois-Jaarsma, Q. (2020). *Regulation of neurotransmitter release by C-domain Ca<sup>2</sup>-sensors*. [PhD-Thesis - Research and graduation internal, Vrije Universiteit Amsterdam].

### **General rights**

Copyright and moral rights for the publications made accessible in the public portal are retained by the authors and/or other copyright owners and it is a condition of accessing publications that users recognise and abide by the legal requirements associated with these rights.

- Users may download and print one copy of any publication from the public portal for the purpose of private study or research.
- You may not further distribute the material or use it for any profit-making activity or commercial gain
- You may freely distribute the URL identifying the publication in the public portal ?

### **Take down policy**

If you believe that this document breaches copyright please contact us providing details, and we will remove access to the work immediately and investigate your claim.

### **E-mail address:**

[vuresearchportal.ub@vu.nl](mailto:vuresearchportal.ub@vu.nl)

# Chapter 6



---

## General discussion

---

### 1. Scope

As introduced in **chapter 1**, release of SVs can be evoked by action potentials or they can be released in their absence. Cytosolic  $\text{Ca}^{2+}$  plays a role in both forms of release. The Double  $\text{C}_2$  proteins (Doc2a/b) contribute to neurotransmitter secretion by acting as a  $\text{Ca}^{2+}$ -dependent regulator of asynchronous <sup>1,2</sup> and spontaneous vesicle fusion (mPSCs or minis) <sup>3,4</sup>. AP-independent  $\text{Ca}^{2+}$ -elevations occur in the presynaptic cytoplasm. We refer to them as spontaneous  $\text{Ca}^{2+}$  elevations (SCEs) because no triggering mechanism has been identified. The intracellular  $\text{Ca}^{2+}$  elevation may originate from extracellular <sup>5</sup>, intracellular  $\text{Ca}^{2+}$ -stores <sup>6,7</sup>. In the latter case, they might also be triggered by GPCR activation (see review <sup>8</sup>). These observations prompted the hypothesis that SCEs may activate  $\text{Ca}^{2+}$  sensor proteins such as Doc2 and trigger spontaneous release. Yet, experimental proof for this hypothesis is lacking and the molecular mechanism driving spontaneous vesicle fusion remains unknown.

This thesis deals with the regulation of synaptic transmission on the two distinct levels: first by fast, spontaneous presynaptic  $\text{Ca}^{2+}$ -signaling and second by various presynaptic  $\text{Ca}^{2+}$ -sensing  $\text{C}_2$  domain proteins. The overall aim of this work described was to gain insight in the presynaptic mechanisms underlying regulation of spontaneous release, synaptic strength and plasticity.

#### 1.1. Main findings

In **chapter 2**, we investigated the frequency and kinetic characteristics of SCEs in resting neurons using genetically encoded  $\text{Ca}^{2+}$ -indicators. Recent advances in live  $\text{Ca}^{2+}$  imaging offer unprecedented spatial and temporal resolution, which facilitates the detection of SCEs but also engenders an unmet need for data processing. The local and short-lived nature of SCEs, together with their low amplitude and frequency make the detection of these events challenging and their analysis by existing open source programs <sup>9,10</sup> unsuitable for this purpose. Therefore, a MATLAB based analysis method was developed to automatically identify rapid  $\text{Ca}^{2+}$  rises in without predetermined regions of interest. The algorithm detected low-amplitude signals with various waveforms in noisy time lapse imaging data. Using a fast variant of GCaMP6 (GCaMP6f), the most common class of  $\text{Ca}^{2+}$  elevations, named SCTs (for spontaneous  $\text{Ca}^{2+}$  transients), exhibited fast kinetics with a mean Full Width at Half Maximum (FWHM) of 0.278 and an SD of 0.146 s. The signal amplitude was faint (mean  $\Delta\text{F}/\text{F}_0 = 0.064$ ; SD = 0.011) and the SCTs occurred with variable frequencies of 0.174 Hz (mean; SD=0.322 Hz).

The reliability of the method was confirmed using both simulated and experimental data by testing its detection sensitivity using experimental data and simulated experiments with various SNRs. The availability of this method is highly valuable to speed up future investigations studying the role of SCEs in neuronal cells or circuits.

The method was employed in **chapter 3** to investigate if stochastic  $\text{Ca}^{2+}$  fluctuations could potentially cause spontaneous neurotransmitter release events. Spontaneous release probability is regulated by  $[\text{Ca}^{2+}]_e$ <sup>3-5,11</sup> and intracellular  $\text{Ca}^{2+}$ <sup>12,13</sup>, but it is unclear if these effects are primarily attributable to global  $[\text{Ca}^{2+}]_i$ , SCEs, or both. We thus explored  $\text{Ca}^{2+}$  transients in glutamatergic hippocampal neurons by simultaneous electrophysiology and high-speed  $\text{Ca}^{2+}$  imaging using different  $\text{Ca}^{2+}$  probes. Among the  $\text{Ca}^{2+}$  reporters tested, SyGCaMP6f appeared the most efficient for the detection of presynaptic SCEs. Besides the fast SCTs, we also observed a variety of other SCE waveforms. An increase in extracellular  $\text{Ca}^{2+}$  caused an increase in global  $[\text{Ca}^{2+}]_i$  as expected, but also increased the frequency of dynamic  $\text{Ca}^{2+}$  elevations. This primarily affected complex  $\text{Ca}^{2+}$  events. mEPSCs detected by patch-clamp recording were not time-locked to SCTs and SCEs. This suggests that quantal glutamate release is either regulated by global  $[\text{Ca}^{2+}]_i$  or that SCEs induce SV secretion with a slow (>1s) or variable delay.

In **chapter 4**, we addressed the mechanism of Doc2b function which was postulated to act as a  $\text{Ca}^{2+}$  sensor<sup>3</sup> or as a structural element supporting  $\text{Ca}^{2+}$ -dependent secretion<sup>4</sup>. Both studies relied on the effects of  $\text{Ca}^{2+}$  binding site mutants, named Doc2b<sup>DN</sup> and Doc2b<sup>6A</sup>. We therefore explored spontaneous and evoked release modification in a side-by-side comparison of Doc2b<sup>WT</sup>, Doc2b<sup>DN</sup> and Doc2b<sup>6A</sup>. We found that the neutralization of critical aspartates had similar gain of function effects on the spontaneous release frequency at rest, which paralleled *in vitro* plasma membrane binding characteristics, reinforcing the idea of its action as a  $\text{Ca}^{2+}$  sensor. In addition, our results suggest that both mutants enhance the synaptic release probability ( $P_r$ ) upon single AP stimulations, thereby affecting short-term plasticity and EPSC rundown during prolonged stimulation. This chapter also supports the idea that Doc2b contributes to synaptic recovery and potentiation in a manner that requires  $\text{Ca}^{2+}$  binding.

In **chapter 5**, we further investigated the synaptic mechanism responsible for the residual spontaneous secretion in absence of the main sensors for quantal release. As candidates we selected three  $\text{C}_2$  domain proteins based on their high similarity with Doc2a and b: Doc2c, rabphilin-3a and Synaptotagmin-7 (Syt-7). Despite their high resemblance with Doc2a & b, gene inactivation of Doc2c and Syt-7 did not influence spontaneous release in excitatory hippocampal neurons. Rabphilin seemed to inhibit spontaneous release frequency in networks but this activity did not appear in autaptic culture. Our findings narrow down the repertoire of potential synaptic  $\text{Ca}^{2+}$  sensors for spontaneous release and redirect our interest to other  $\text{C}_2$  domain proteins.

## 2. $\text{Ca}^{2+}$ signaling of spontaneous release

### 2.1. Temporal characterization of $\text{Ca}^{2+}$ transients

In presynaptic terminals, the intracellular  $\text{Ca}^{2+}$  concentration profile during AP-induced VGCC activation is characterized by highly local peaks immediately adjacent to the  $\text{Ca}^{2+}$  channels. The local nature of these  $\text{Ca}^{2+}$  signals matches a remarkably well organized subcellular architecture<sup>14</sup> (for review<sup>15,16</sup>). The nanoscale topography of  $\text{Ca}^{2+}$ -channels relative to synaptic vesicles ensures rapid neurotransmission upon AP arrival. Thus, the delay time between  $\text{Ca}^{2+}$ -entry and synaptic vesicle fusion is extremely short. A number of investigations reported a synaptic delay of  $\sim 1$  ms (presynaptic AP to postsynaptic AP) and  $\text{Ca}^{2+}$  triggers vesicle fusion and neurotransmitter release in a few hundred of milliseconds<sup>17–21</sup>. Pioneering works studied the process at the NMJ<sup>20</sup>, rat cerebellar fiber synapse<sup>22</sup> and the Calyx of Held synapse<sup>23,24</sup>. Simultaneous pre- and postsynaptic electrophysiological recordings in the squid giant synapse and mathematic isolation of the  $\text{Ca}^{2+}$ -current estimated a latency between the inward  $\text{Ca}^{2+}$  current and transmitter release of  $\sim 200$   $\mu\text{s}$ <sup>17</sup>. In chapter 3 (Chapter 3, Figure 7A-B), we measured the latency between the presynaptic  $\text{Ca}^{2+}$ -influx monitored by presynaptically targeted GECI sy-GCaMP6f and the AP evoked EPSC peak signal. The delay of the reported  $\text{Ca}^{2+}$  entry relative to the postsynaptic activation in our hands appeared to be +50 to +150 ms, meaning that the detection appeared after the EPSC, which is clearly a technical issue. Yet, electrophysiology and imaging acquisitions were precisely synchronized (Chapter 3, Figure S4) using internal controls which confirm accurate timestamping in the EMCD camera (an accuracy of  $\sim 10$  ns is specified by the manufacturer). The delay in fluorescent peak detection is longer than described by purely electrophysiological approaches<sup>17,25,26</sup>. The mismatch could be explained by the association kinetics of  $\text{Ca}^{2+}$  ions to the fluorescent indicators. Other studies with fluorescent  $\text{Ca}^{2+}$  indicators also report longer latencies than electrophysiological measurements. Previously reported measurements using OGB-1 exhibited a latency around 320 ms<sup>10</sup>. The  $\text{Ca}^{2+}$  peak FWHM triggered by a single AP with OGB-1 in our study was 176 ms (Chapter 3, Table 1). For GCaMP6f, the fastest GECI available, previous studies showed a FWHM of 360 ms and a time to peak latency from 50 to 75 ms<sup>27</sup> for a single AP. The association kinetics importantly depend on the  $[\text{Ca}^{2+}]$ . For GCaMP1, the  $\text{Ca}^{2+}$  association time constant ranges broadly from 230 ms at 0.2  $\mu\text{M}$   $\text{Ca}^{2+}$  to 2.5 ms at 1  $\mu\text{M}$   $\text{Ca}^{2+}$ <sup>28</sup>, while the dissociation constant was not affected by  $[\text{Ca}^{2+}]$ .

Another indication that fluorescent indicators markedly delay the  $\text{Ca}^{2+}$  peak signal can be deduced from a direct comparison of data obtained with GCaMP6f versus OGB-1. For low  $[\text{Ca}^{2+}]$  amplitude SCTs, OGB-1 signals had a FWHM of  $\sim 49$  ms (Table 1) compared to  $\sim 260$  ms for GCaMP6f (Chapter 3, Stat. table 6 & Figure 6). The ratio of these FWHM values indicates that OGB-1 is a  $\sim 5.75$  fold faster reporter than GCaMP6f. Thus, in the full chain of events from  $\text{Ca}^{2+}$  channel opening to optical measurement of  $\text{Ca}^{2+}$  induced fluorescence signals and dynamics, the delay from binding of  $\text{Ca}^{2+}$  onto the indicator to the emergence of fluorescence forms a profound rate-limiting step. In contrast, imaging framerates were not rate-limiting in our experiments, while channel dynamics and  $\text{Ca}^{2+}$  diffusion have minor effects. Altogether, before performing  $\text{Ca}^{2+}$ -imaging, it must be taken into consideration that

$\text{Ca}^{2+}$  signals are optically reported with a delay which is an inherent property of the  $\text{Ca}^{2+}$  indicator used. The delay also varies with the nature of the  $[\text{Ca}^{2+}]$  signal. It would be helpful if a next generation GECIs could be improved to achieve shorter latencies close to that of chemical  $\text{Ca}^{2+}$ -probes, allowing to detect  $\text{Ca}^{2+}$  events at a higher temporal resolution while retaining possibilities for subcellular targeting.

The image acquisition speed is also an important parameter. In our experiments the framerate of  $\sim 30$  Hz was more than sufficient for accurate detection of  $\text{Ca}^{2+}$ -events, which had a mean peak width (FWHM) of  $\sim 8$  frames (FWHM = 278 ms and acquisition every 33 ms).

## 2.2. Spatial characterization of $\text{Ca}^{2+}$ transients in relation to spontaneous release

The ultrastructure and topology of presynaptic protein architectures have started to elucidate how scaffold proteins establish nanodomains that connect VGCCs with release-ready SVs in a radius of approximately 30 nm<sup>29</sup> (Chapter 1, see Figure 1). Scaffold proteins seem to operate as molecular linkers, limiting SV-VGCC distances to tens of nanometers, thereby regulating the probability and plasticity of SV release<sup>30</sup>. Measurements of quantal secretion have shown that the vesicular release probability decreases threefold with a doubling of the distance between the  $\text{Ca}^{2+}$  channel and the synaptic vesicle from 25 to 50 nm<sup>31</sup>.

In chapter 3,  $\text{Ca}^{2+}$ -transients emerged all over the neuron which led to the idea that they might appear in an unpredictable spatial pattern. Deeper analysis of GCaMP6f fluorescence revealed that 70% of the SCTs co-localize with synapsin-eGFP. In line with this, Sy-GCaMP6f detected 2.5-fold more SCT events compared to global GCaMP6f (Chapter 3; Figure 5) which suggests a spatial enrichment of fast transients in the presynaptic element.

Various  $\text{Ca}^{2+}$  sources have been observed to affect the frequency of mPSCs: 1. Intracellular stores, from which  $\text{Ca}^{2+}$  can be liberated through  $\text{IP}_3\text{R}$  and/or RyR channels<sup>7,32</sup>, 2. The spontaneous opening of VGCC at the resting potential, also referred to as VGCC flickering<sup>5,33</sup>. Those two mechanisms can generate global  $[\text{Ca}^{2+}]_i$  fluctuations depending on the equilibrium between  $\text{Ca}^{2+}$  liberation and  $\text{Ca}^{2+}$  buffering and clearance. Caffeine application<sup>32,34</sup> and  $[\text{Ca}^{2+}]_e$  increase<sup>35</sup> are well described and commonly increase spontaneous release. Application of an agonistic caffeine concentration significantly increased the SCT frequency from 0.23 Hz to 0.36 Hz (Chapter 2, Figure 6). These data support the implication of intracellular  $\text{Ca}^{2+}$ -stores in the generation of presynaptic  $\text{Ca}^{2+}$ -transients but do not rule out the possible involvement of extracellular sources. Prior works revealed the involvement of the  $\text{Ca}^{2+}$ -induced  $\text{Ca}^{2+}$ -release mechanism in spontaneous release<sup>6</sup>. This mechanism was shown to be critical for the amplification of faint  $\text{Ca}^{2+}$ -events in the postsynaptic element<sup>36</sup>. Extracellular  $[\text{Ca}^{2+}]_e$  rise from 0 mM to 10 mM promoted the frequency of both mEPSCs and SCEs (Chapter 3, Figure 4 & 6). The same treatment also caused an increase in global  $[\text{Ca}^{2+}]_i$  as confirmed by Fura-2 imaging (Chapter 3, Figure 4). The concomitant increase in global  $[\text{Ca}^{2+}]_i$  may be a direct consequence of the increased  $[\text{Ca}^{2+}]_e$ , implying a passive  $\text{Ca}^{2+}$  leakage following the concentration gradient, or an indirect result of the higher SCE frequency.

In both cases, the limited  $\text{Ca}^{2+}$  clearance capacity likely yields a progressive cytosolic build-up, coercing the cell to a higher  $[\text{Ca}^{2+}]_i$  steady state (Chapter 3, Figure 4B). In Chapter 2 and 3, complex  $\text{Ca}^{2+}$  transients were described as all events lasting longer than 280 ms, usually covering larger areas than SCTs and forming very different waveforms. This may suggest the existence of multiple triggering mechanisms. In the GCaMP6f experiments, complex events represented 43% of all events (Chapter 2). They were frequent in the presynaptic compartment (0.082 Hz vs 0.13 Hz for GCaMP6f vs SyGCaMP6f respectively; Chapter 3, Figure 5) and their frequency was affected more by extracellular  $[\text{Ca}^{2+}]_e$  than that of SCTs (Chapter 3, Figure 6). SCEs could either arise from the summation of SCTs by simultaneous channel unit opening or via the CICR amplification mechanism. Further investigations are necessary to disclose the pathway driving SCEs.

Altogether, our data support the preferential involvement of long lasting, complex  $\text{Ca}^{2+}$  fluctuations rather than fast SCTs in SV fusion in resting glutamatergic hippocampal neurons. The observation that caffeine increases the frequency of TTX-insensitive SCTs, together with the preferential involvement of SCEs in spontaneous release suggests that the CICR mechanism is also functional in the presynapse for minis.

### 2.3. $\text{Ca}^{2+}$ dose-dependence of spontaneous release

Many investigations attempted to precisely measure the  $\text{Ca}^{2+}$  dependence of neurotransmitter release. A wide range in  $\text{Ca}^{2+}$  affinities of evoked and spontaneous release were reported, likely because of the variety in methodologies used and the different brain structures investigated. Early studies investigated the relationship between intraterminal  $[\text{Ca}^{2+}]_i$  using a combination of  $\text{Ca}^{2+}$ -indicators during photolysis of caged  $\text{Ca}^{2+}$ , ionomycin perfusion and either intracellular electrophysiology or capacitance measurements. Ratiometric Fura-2 imaging and intracellular recording of miniature end plate potentials (MEPPs) at the frog neuromuscular junction reported a resting  $[\text{Ca}^{2+}]_i$  of around ~100 nM together with marked increase in the frequency of MEPPs at 500 nM <sup>37</sup>. Caged  $\text{Ca}^{2+}$  photolysis <sup>38</sup> and ionomycin application <sup>39</sup> methods yielded lower  $\text{Ca}^{2+}$ -sensitivities for synchronous and asynchronous release than for spontaneous release. In the Calyx of Held, a combination of ratiometric and non-ratiometric  $\text{Ca}^{2+}$  probes indicated a resting  $[\text{Ca}^{2+}]_i$  of 40 nM and a peak amplitude of  $\text{Ca}^{2+}$  transients elicited by single APs around 400 nM to 500 nM <sup>40</sup>. In apical dendrites of hippocampal CA1 neurons, resting  $[\text{Ca}^{2+}]_i$  was evaluated by OGB-1 imaging to be 32 nM to 59 nM and monitoring evoked  $\text{Ca}^{2+}$  transients yielded estimates of peak  $[\text{Ca}^{2+}]_i$  of 178 nM to 312 nM <sup>41</sup>. As the availability of the  $\text{Ca}^{2+}$ -indicators diversified, the use of Fluo-4 together with OGB-1 highlighted the importance of endogenous  $\text{Ca}^{2+}$  buffering capacity and subcellular volume which influence the  $[\text{Ca}^{2+}]_i$  peak during single APs (respectively  $528 \pm 251$  nM in the spine and  $401 \pm 139$  nM in the dendrite) <sup>42</sup>. The  $[\text{Ca}^{2+}]_{\text{rest}}$  in individual giant mossy fiber boutons was evaluated to  $116 \pm 20$  nM with Fluo-4 and  $103 \pm 14$  nM with OGB-1 <sup>43</sup>. A later study estimated a much higher peak  $\text{Ca}^{2+}$  concentration at the VGCC mouth of approximately 100  $\mu\text{M}$  during evoked neurotransmitter release <sup>29</sup>, likely due to the advancement of temporal and spatial resolution. It stands out that reported  $\text{Ca}^{2+}$ -event properties differ depending on the spatial (subcellular compartment or whole cell) and temporal focus of the study.



Altogether, the  $\text{Ca}^{2+}$  rise following a single action potential is approximately 5- to 10-fold higher than resting  $\text{Ca}^{2+}$  concentration. In our hands, OGB-1 reported a 4-fold increase in the  $\Delta F/F_0$  peak signal during a single AP compared to the amplitude of spontaneous events (Chapter 3, Table 2).

The contrast between the low-threshold  $\text{Ca}^{2+}$  requirement for spontaneous release and the high  $\text{Ca}^{2+}$  threshold of fast evoked release is striking. The different phases of release, namely spontaneous, asynchronous and synchronous release arise along a wide range of  $[\text{Ca}^{2+}]$  and show a  $\text{Ca}^{2+}$ -sensitivity from 50 nM to 50  $\mu\text{M}$  in the Calyx of Held, however with different  $\text{Ca}^{2+}$ -cooperativity<sup>44-46</sup>. Taken together, the  $[\text{Ca}^{2+}]_i$  window in which a  $\text{Ca}^{2+}$ -sensor could exert its function for spontaneous SVs fusion can be situated above the resting  $\text{Ca}^{2+}$  concentration of 40-50 nM and below the activation threshold of evoked release around 400-500 nM. Considering concordant reported values of absolute peak  $[\text{Ca}^{2+}]$  during a single AP (in average  $\sim 387$  nM), together with our comparison with the  $\Delta F/F_0$  obtained from OGB-1 imaging (Chapter 3, Table 1&2), one can estimate an absolute peak  $[\text{Ca}^{2+}]$  during SCTs of  $\sim 121$  nM. This estimate is coherent with the high  $\text{Ca}^{2+}$ -affinities of membrane binding activity by identified  $\text{Ca}^{2+}$  sensors for spontaneous release Doc2a, b ( $\text{EC}_{50}$  of respectively 450 nM and 175 nM, Chapter 4)<sup>47</sup>.

## 2.4. The $\text{Ca}^{2+}$ trigger of Doc2

Doc2 is the main sensor involved in quantal neurotransmitter release, yet the relation of Doc2b driven spontaneous release with the  $\text{Ca}^{2+}$ -source is not resolved. Based on its high  $\text{Ca}^{2+}$ -sensitivity<sup>47</sup> and considering that Syt-1 activation requires higher  $[\text{Ca}^{2+}]$  ( $\text{EC}_{50} \sim 3.5 \mu\text{M}$ )<sup>48,49</sup> it is very likely that Doc2b is specifically activated by  $\text{Ca}^{2+}$  levels that do not activate Syt-1. As suggested by our investigation in chapter 3, both global cytosolic  $\text{Ca}^{2+}$  and SCEs potentially control quantal release but the portion of Doc2b-driven release events in these assays isn't known. Unlike Syt-1, Doc2 is a cytosolic protein with no physical association to  $\text{Ca}^{2+}$  microdomains, as far as known. This feature may render Doc2 activatable by  $\text{Ca}^{2+}$  events that occur at distinct locations relative to Syt-1. Being associated to vesicles, Syt-1 is preferentially activated by  $\text{Ca}^{2+}$ -influx through VGCCs. The localization of Doc2b is likely more dynamic: it has several interactors that can target it to release sites. The N-terminal MID enables its co-translocation with Munc13 to the plasma membrane<sup>50-52</sup>. This activation pathway is stimulated by phospholipase C-dependent production of diacylglycerol, which can be mimicked experimentally by phorbol ester administration<sup>51</sup>. The Doc2b-Munc13 association mechanism promotes vesicle release and synaptic augmentation<sup>53</sup>. Doc2b also associates with the SNARE-accessory protein Munc18<sup>54,55</sup> and the SNARE proteins syntaxin-1 and SNAP25<sup>3</sup>, providing another pathway for Doc2b release site targeting. Therefore, global cytosolic  $\text{Ca}^{2+}$  increases might enhance Doc2b-driven quantal release via the PLC / DAG /  $\text{IP}_3$  / Munc13 association pathway (Chapter 1, Figure 5), whereas  $\text{Ca}^{2+}$  transients caused by VGCC flickering could directly trigger Doc2b molecules already present near the exocytotic apparatus. The latter idea may not be relevant for mouse hippocampal GABAergic neurons, because mIPSC events sensitive to  $\text{Cd}^{2+}$  blockade of VGCCs are Doc2b-independent<sup>56</sup>. Yet, this pathway might occur in other cell types. Further investigations are necessary to clarify the specific  $\text{Ca}^{2+}$  trigger for Doc2 driven spontaneous release.

## 2.5. Limitations to our study of SCE – mEPSC correlation

In chapter 3 of this thesis, we investigated the relation between spontaneous neurotransmitter release and presynaptic  $\text{Ca}^{2+}$ -events. The temporal correlation between SCEs and mEPSCs appeared poor at high  $[\text{Ca}^{2+}]_e$  (Chapter 3, Figure 4 & 6). Refined analysis of the temporal correlation of mEPSCs relative to single or complex events at 4 mM  $[\text{Ca}^{2+}]_e$  (Chapter 3, Figure 7 & 8) led to a similar conclusion. Yet, a parallel increase of cytosolic  $\text{Ca}^{2+}$  and minis was reported multiple times<sup>7,37</sup>. Several technical and physiological limitations could cause a hypothetical coupling between SCEs and mEPSC to remain undetected. The first technical limitation relies on the  $\text{Ca}^{2+}$  indicator performance. The latency from AP-induced  $\text{Ca}^{2+}$  peak and the EPSC was mentioned earlier to be in order of 50 to 150 ms with the GCaMP6f. We took this delay into account in our temporal analysis, by inspecting minis in a time window of 250 ms and 1 s before and after  $\text{Ca}^{2+}$  transients. However, the slow  $\text{Ca}^{2+}$ -association kinetics of the GECl, particularly for low peak  $[\text{Ca}^{2+}]_i$ , could then leave fast SCTs undetected<sup>28</sup>. Indeed, low  $\text{Ca}^{2+}$  binding affinity and slow kinetic can give enough time for endogenous  $\text{Ca}^{2+}$  buffering, extrusion and diffusion mechanisms to clear intracellular  $\text{Ca}^{2+}$  before it can bind the fluorescent reporter. The second restriction could arise from the imaging methodology. The imaging field of view was roughly ~70% smaller than the entire autaptic neuron, which is expected to lead to a proportional reduction of detected SCEs (but not mEPSCs).

Moreover, GCaMP6f associates with  $\text{Ca}^{2+}$  with a  $K_d$  around 375 nM<sup>27</sup> which means that small  $\text{Ca}^{2+}$  elevations below this threshold could remain undetected. Yet, quantal release is at least partially driven by high affinity sensors as Doc2b which show an  $\text{EC}_{50}$  around 175 nM. Therefore, one can envision that low-amplitude SCEs escape detection, but trigger spontaneous SV fusion.

The last restriction could relate to different mechanisms for spontaneous release in excitatory vs. inhibitory synapses<sup>33,56–58</sup>. Spontaneous fusion events appear preferentially triggered by local  $\text{Ca}^{2+}$  micro-domains generated via stochastic openings of VGCCs only at GABAergic, but not glutamatergic terminals<sup>33</sup>. Selective and unselective VGCC blockers affected mIPSC but not mEPSC frequency in neocortex neurons<sup>58</sup>. A recent investigation reported the preferential involvement of Syt-1 in spontaneous GABA release<sup>56</sup>, consistent with the strategic location of the fast sensor nearby VGCCs in support of quantal GABA release. In contrast, spontaneous release frequency was altered by  $[\text{Ca}^{2+}]_e$  and both EGTA and  $\text{Cd}^{2+}$  at cholinergic and GABAergic synapses at *C. Elegans* NMJ<sup>57</sup>. Both mEPSCs and mIPSCs were shown to rely on  $\text{CaV}_1$  and  $\text{CaV}_2$  channel opening. mIPSCs exhibited a higher proportion of  $[\text{Ca}^{2+}]_e$ -independent events than mEPSCs as suggested by the effect of EGTA and  $\text{Cd}^{2+}$ <sup>57</sup>. Thus, spontaneous release seems to be, at least in part, differently regulated at excitatory and inhibitory synapses. In Chapter 3 where we observed no tight coupling between SCEs and mEPSCs, our investigations were performed on excitatory hippocampal neurons, while only a minority of GABAergic neurons was present in the culture. It is thus important to note that the lack of tight coupling cannot be extrapolated to inhibitory neurons.

In conclusion, an accurate time correlation between  $\text{Ca}^{2+}$ -transients and vesicle fusion at rest may possibly have remained undetected if the triggering signal would rely on an extremely rapid, low amplitude  $\text{Ca}^{2+}$ -peak, considering the technical limits of available tools. To acquire more certainty, this quest would be facilitated by the use of improved indicators with faster  $\text{Ca}^{2+}$  association kinetics that simultaneously report  $\text{Ca}^{2+}$  and fusion events.

## 2.6. Spatial correlation of synaptic vesicle fusion and SCTs

### The all-optical alternative

As an alternative approach, an all optical technique can be employed to assess presynaptic  $\text{Ca}^{2+}$ -signalling together with synaptic release events. This method requires indicators with appropriate excitation and emission wavelengths to simultaneously detect synaptic fusion and  $\text{Ca}^{2+}$  events. Optical methods for synaptic vesicles trafficking at the active zone have been developed using a pH-sensitive GFP fluorophore termed pHluorin<sup>59</sup>. pHluorin can be targeted to the synaptic vesicle lumen by fusion to synaptophysin (syphHy)<sup>60</sup> or other vesicle associated proteins. It is quenched by the low acidic pH in the vesicles but the fluorescence increases as the vesicles fuse with the PM, neutralizing the pH due to content mixing with the extracellular environment. Fusion events are identified as a sudden brightness increase in syphHy fluorescence which declines upon vesicle re-acidification following endocytosis.

Dual channel detection of  $\text{Ca}^{2+}$  and SV secretion has been achieved using GCaMP3 as  $\text{Ca}^{2+}$  indicator in the green emission channel, combined with red-shifted variants of syphHy as indicators for vesicle fusion. Examples of the latter are VGLUT-mOr2<sup>61</sup> or SyphHyTomato<sup>62</sup>. An alternative approach uses the red shifted calcium indicator R-GECO1<sup>63</sup> and syphHy in a unique probe syphHy-RGECO<sup>64</sup> respectively targeted to the intracellular space and the vesicular lumen. This enables to simultaneously track  $\text{Ca}^{2+}$ -events and concomitant vesicular fusion with a single-molecule indicator. Our laboratory recently developed a new imaging fluorescent probe, syphHyJREx, made of syphHy and JREx, a red-shifted  $\text{Ca}^{2+}$  indicator developed from REX-GECO1<sup>65</sup>. pHluorin located in the vesicle lumen and JREx on the cytoplasmic outer surface are excited with the same wavelength (480 nm) but their emission peaks occur respectively at 510 and 585 nm. This allows to report  $\text{Ca}^{2+}$ -secretion coupling by simultaneous dual channel imaging. The slow  $\text{Ca}^{2+}$ -association kinetics of the GECIs will still cause a delay, but on the other hand, optical detection offers the advantage of providing spatial information. The invasiveness of neuronal stimulation can also be overcome by optical stimulation methods. For example, the red-shifted channelrhodopsin Chrimson<sup>66</sup> gives promising perspectives for photostimulation in combination with the detection of  $\text{Ca}^{2+}$  and vesicle fusion events.

To summarize all the above, our investigation in hippocampal excitatory neurons yielded new insights in the various types of spontaneous  $\text{Ca}^{2+}$  fluctuations that occur during rest in the presynaptic compartment. Although our methods do have some limitations, we did not detect a tight temporal coupling of quantal fusion events to SCEs. Several mechanistic models, summarized in Figure 1 (Chapter 6), can explain how  $\text{Ca}^{2+}$  may regulate spontaneous release. The contributions of each of these mechanisms remain to be investigated in the future.

### 3. Mechanism(s) of spontaneous release

#### 3.1. Functional diversity of C<sub>2</sub> domains

In this research project different proteins containing similar C<sub>2</sub> domain architectures were investigated using the same methodology (see Chapter 5). C<sub>2</sub> domains typically form independent Ca<sup>2+</sup>-binding modules<sup>67</sup> that endow Ca<sup>2+</sup>-dependent lipid binding properties to the protein. However, as an exception to this typical pattern, some C<sub>2</sub> domains have diverged evolutionarily into Ca<sup>2+</sup>-independent forms<sup>67</sup> suggesting that C<sub>2</sub> domains also have other functions. Ca<sup>2+</sup>-independent isoforms of protein kinase C such as PKC  $\delta$  and  $\theta$  lack Ca<sup>2+</sup>- and phospholipid binding, but instead bind phosphotyrosine instead<sup>68,69</sup>, providing an alternative activation mechanism. As a second example, the Syt-12 isoform which colocalizes with Syt-1 on synaptic vesicles does not bind Ca<sup>2+</sup>, but its overexpression still specifically increases spontaneous release in cultured neurons<sup>70</sup>. This suggests that C<sub>2</sub> modules provide Ca<sup>2+</sup>-independent secretory functions. The third member of the Doc2 protein family, Doc2c, despite its high amino acid sequence identities with Doc2a and b (45.6 % and 43.2% respectively), does not contain Ca<sup>2+</sup>-dependent phospholipid binding activity<sup>71</sup> nor associates with the PM in response to Ca<sup>2+</sup> influx<sup>47,71</sup>. Doc2c contains a unique highly basic sequence<sup>177RLRRRRRR<sup>183</sup></sup>, situated in the CBL3 of the C<sub>2</sub>A domain<sup>72</sup>, that could theoretically support Ca<sup>2+</sup>-independent interactions with negatively charged membranes. In chapter 5, we show that Doc2c is not involved in spontaneous (Chapter5, Figure 2) or evoked (Chapter 5, Figure 3) neurotransmitter release in absence of the main sensors for spontaneous release in hippocampal neurons. This is in line with the lack of conservation of critical aspartate residues in its C<sub>2</sub>A domain. Most proteins with C<sub>2</sub> domains function in signal transduction or membrane traffic, e.g. for the generation of lipid second messengers or exocytosis. Whereas Doc2c does not function in glutamate exocytosis, we cannot rule out a role in other secretory processes.

The conserved amino acid sequence of the C<sub>2</sub>B domain suggests it might still bind Ca<sup>2+</sup> whereas the C<sub>2</sub>A domain may act as Ca<sup>2+</sup>-independent targeting module for the protein (see review)<sup>73</sup>. Quantitative single cell RT-PCR revealed substantial Doc2c co-expression together with Doc2a,b in cultured hippocampal neurons<sup>74</sup>. The MID domain sequence is also fully conserved meaning that the DAG-dependent Munc13 association is functional. It could be hypothesized that Doc2c acts on vesicle trafficking through the regulation of Munc13. The basic amino acid sequence in the Doc2c's C<sub>2</sub>A domain has been proposed to function as a nuclear localization signal<sup>72</sup> which targets Doc2c to the nucleus<sup>47,72</sup>. Mouse transcriptome data indicates that it is highly expressed in the heart<sup>75</sup>, unlike other Doc2s. Cardiac myocytes present cytosolic ([Ca<sup>2+</sup>]<sub>cyt</sub>) and nuclear [Ca<sup>2+</sup>] ([Ca<sup>2+</sup>]<sub>nuc</sub>) oscillations which respectively control the beat-to-beat contractile activation and gene expression<sup>76</sup>. Both activities converge to an excitation-transcription feedback loop that integrates contractile activity for adequate cardiomyocyte reprogramming. Thus, in the heart, Doc2c activation via C<sub>2</sub>B could conceivably contribute to nuclear envelope dynamics or gene expression reprogramming. In Chapter 5, we reported the first knock-out mice model for Doc2c, which are viable and display no sign of major impairment in neural functions or survival. Therefore, its hypothesized activity cannot be essential for vital aspects of brain and heart function.

Another difference observed in different C<sub>2</sub> domains is the nature of the change induced by Ca<sup>2+</sup>-binding. Electrostatic modifications are considered to be the major contributor to C<sub>2</sub> domain activation of Syts<sup>77–79</sup> and Doc2b<sup>80</sup>. In addition, hydrophobic interactions support membrane penetration of loops extending out of the Ca<sup>2+</sup>-binding site. Yet, a long variant of piccolo's C<sub>2</sub>A domain<sup>81,82</sup> and the CBL1 in the C<sub>2</sub>A domain of rabphilin-3A<sup>83</sup> undergo significant conformational changes upon Ca<sup>2+</sup>-binding. The Piccolo long variant shows low Ca<sup>2+</sup> affinity, which is increased in the short C<sub>2</sub>A variant<sup>82</sup>, suggesting that a conformational difference directly affects the Ca<sup>2+</sup> affinity. In both PCLO and rabphilin, the backbone and side chains of the Ca<sup>2+</sup>-binding aspartates adopt conformational modifications that have been observed in structural studies of the Ca<sup>2+</sup>-free/bound structures by NMR and X-ray crystallography.

Thus, the range of C<sub>2</sub> domain activation mechanisms seems more broad than previously thought. Many C<sub>2</sub> domains show limited conformational variations upon Ca<sup>2+</sup> binding, likely due to the compact arrangement of C<sub>2</sub> domains together with other fusogenic proteins, which may not permit conformational changes. Another conclusion is that slight structural modifications from one C<sub>2</sub> domain to another may account for important functional changes and biophysical properties. Given the significant differences in their mode of action, it is important to specifically consider each protein in the context of structural models for their activity.

### 3.2. C<sub>2</sub>A and C<sub>2</sub>B domains: role in phospholipid binding and membrane fusion

There is an important distinction to make between single C<sub>2</sub> domain proteins (e.g. PKC, PLC) and multiple tandem C<sub>2</sub> domains (Syts, Doc2). Single C<sub>2</sub> domains regulate protein membrane targeting and activity<sup>84</sup> whereas tandem C<sub>2</sub> domains have an additional activity in inducing membrane deformation, which contributes to the regulation of membrane fusion probability together with the SNARE-dependent activities<sup>85–89</sup>. It has been reported that tandem C<sub>2</sub> domains in close proximity are necessary to bridge opposing membranes in contrast to individual C<sub>2</sub> domains that fail to trigger membrane cross-linking<sup>77,90</sup>. Accordingly, the activity of Syt-1 C<sub>2</sub> domains to induce membrane curvature and fusion requires that the C<sub>2</sub>A and C<sub>2</sub>B domains are linked to each other in tandem<sup>87</sup>. The presence of two or more C<sub>2</sub> domains in proteins enhance the membrane- and Ca<sup>2+</sup>-binding affinity beyond that of individual C<sub>2</sub> domains. Syt-1 tandem C<sub>2</sub> domains were shown to Ca<sup>2+</sup>-dependently penetrate deeper into the membrane bilayer compared to individual C<sub>2</sub>A and C<sub>2</sub>B, suggesting cooperativity<sup>85,91</sup> and Syt-7 tandem C<sub>2</sub>AB binds liposomes with greater Ca<sup>2+</sup>-sensitivity than individual domains<sup>92</sup>. Additionally, Syt-1 C<sub>2</sub>AB dissociates from PIP<sub>2</sub>-free liposomes much more slowly than either of its individual C<sub>2</sub> domains and Syt-7. Therefore, tandem C<sub>2</sub>A and C<sub>2</sub>B domains do not act independently but influence their mutual membrane penetration by cooperative energetic effects.

Isolated and tandem C<sub>2</sub> domains of Syts and Doc2s present different Ca<sup>2+</sup>- and phospholipid-binding properties. Quantitative measurements of the Ca<sup>2+</sup> dose-dependency of phospholipid binding by Syt-1 C<sub>2</sub> domains have yielded various estimates, which strongly depend on the

lipid composition. The  $\text{Ca}^{2+}$ -sensitivity of the  $\text{C}_2\text{B}$  domain appeared higher than that of the  $\text{C}_2\text{A}$ .  $\text{PIP}_2$  binding to the  $\text{C}_2\text{B}$  domain increases the  $\text{Ca}^{2+}$ -sensitivity and strongly influences the sensitivity of full length Syt-1, while  $\text{C}_2\text{A}$  binding is predominantly governed by negatively charged phospholipids<sup>49</sup>. Consistently,  $\text{Ca}^{2+}$  association to the  $\text{C}_2\text{A}$  domain of Syt-1 appears important but not essential for the  $\text{Ca}^{2+}$ -dependent function of the protein<sup>93</sup>, because abrogation of  $\text{Ca}^{2+}$  binding to this domain by mutations (D232N and D238N) did not induce major changes in synaptic transmission. Loss of function mutations in the  $\text{C}_2\text{B}$  domain of Syt-1 have more prominent effects on synaptic transmission than similar mutations in the  $\text{C}_2\text{A}$  domain<sup>85,93–95</sup>. Thus, the  $\text{C}_2\text{B}$  domain is the main determinant for Syt-1-driven  $\text{Ca}^{2+}$ -secretion coupling. Yet, a recent publication reported the absolute requirement of a functional  $\text{C}_2\text{A}$  domain for neurotransmitter release<sup>96</sup>. Mutation of two hydrophobic residues (M224E and F286E) present at the tip of each CBL and adjacent to aspartate residues, abolished release more severely than a Syt-1 null mutation in *Drosophila*<sup>96</sup>. A plethora of mutants was generated in the fast sensor  $\text{C}_2$  domains and their effect on neurotransmitter release was scrutinized. Substitutions in Syt-1, homologous to those in Doc2b, produce different phenotypes<sup>97,98</sup>. D230, 232N neutralization suppressed the  $\text{Ca}^{2+}$  binding activity of the protein<sup>99</sup> and SNARE binding which can be interpreted as a loss-of-function. Neutralization of positively charged residues R233 and K366 present at the membrane binding interface also impaired  $\text{Ca}^{2+}$ -sensitivity for liposome interaction and reduced exocytosis<sup>100</sup>. Similar to mutagenesis in Doc2b, mutations in Syt-1 demonstrated that changing its apparent  $\text{Ca}^{2+}$  affinity for either its phospholipid interactions, or its SNARE binding, altered the apparent  $\text{Ca}^{2+}$  affinity of release<sup>85</sup>.

In Syt-7, the  $\text{C}_2\text{A}$  domain has a much higher  $\text{Ca}^{2+}$ -sensitivity of membrane binding compared to Syt-1  $\text{C}_2\text{A}$ <sup>101</sup>. This high  $\text{Ca}^{2+}$ -sensitivity dominates the phospholipid binding property of full length Syt-7<sup>102</sup>. Quantitative fluorescence measurements revealed a slower dissociation of Syt-7  $\text{C}_2\text{A}$  from lipid bilayers<sup>101</sup>. The crystal structure of Syt-7  $\text{Ca}^{2+}$ -bound  $\text{C}_2$  domains was found very similar to that of Syt-1  $\text{C}_2$  domains<sup>102,103</sup>. Isothermal titration calorimetry (ITC) data also indicate that the intrinsic  $\text{Ca}^{2+}$ -binding properties of Syt-7  $\text{C}_2$  domains are comparable to those of the Syt-1  $\text{C}_2$  domains<sup>102,103</sup>. Altogether, those data do not provide an explanation for the differences in the functional importance of  $\text{C}_2$  domains between Syt-1 and Syt-7. The different behavior of Syt-7 and Syt-1 is ascribed to subtle amino acid substitutions in the  $\text{Ca}^{2+}$  binding interface. In Syt-7,  $\text{Ca}^{2+}$  association to the  $\text{C}_2\text{A}$  domain is the major mediator in asynchronous release<sup>102</sup>.

Also for Doc2b, the apparent  $\text{Ca}^{2+}$  affinities of the  $\text{C}_2$  domains differ from each other and are influenced by the presence of membranes and their phospholipid composition. ITC titrations of isolated  $\text{C}_2$  domains in absence of lipids indicated that only  $\text{C}_2\text{B}$  binds  $\text{Ca}^{2+}$ <sup>104</sup> and was solely responsible for  $\text{Ca}^{2+}$  binding of the  $\text{C}_2\text{AB}$  tandem. In the same study, in presence of lipids,  $\text{C}_2\text{A}$  appeared as the main actuator in the  $\text{Ca}^{2+}$ -dependent liposome association of the  $\text{C}_2$  tandem<sup>104</sup>. Crystal structures of the  $\text{C}_2\text{A}$  and  $\text{C}_2\text{B}$  domains indicated that they accommodate two  $\text{Ca}^{2+}$  ions each with minor conformational changes<sup>80</sup>. In tandem  $\text{C}_2\text{AB}$ , the  $\text{C}_2\text{B}$  domain appeared to be the primary  $\text{Ca}^{2+}$  sensing unit whereas  $\text{C}_2\text{A}$  had an additive effect in enhancing the interaction of  $\text{C}_2\text{AB}$  with the PM<sup>80</sup>.

Similarly, the isolated C<sub>2</sub>A domain binds to liposomes in a Ca<sup>2+</sup> dependent manner while binding of the C<sub>2</sub>B domain is limited<sup>3</sup>. In chapter 4, we measured the apparent Ca<sup>2+</sup>-affinities of phospholipid binding by the C<sub>2</sub>A and C<sub>2</sub>AB domains of Doc2b. The C<sub>2</sub>AB domain showed a drastically higher Ca<sup>2+</sup>-affinity compared to C<sub>2</sub>A (176 nM and 435 nM respectively; Chapter 4, Figure 3) which illustrates the synergistic effect. Aspartate substitutions in the C<sub>2</sub>A domain of Doc2b drive its constitutive PM association<sup>2,104–106</sup>, whereas similar mutations in the C<sub>2</sub>B domain do not<sup>2,104</sup>. Taken together, it is clear that the C<sub>2</sub>A and C<sub>2</sub>B have complementary functions where Ca<sup>2+</sup> activation of soluble Doc2b is likely driven by the C<sub>2</sub>B domain and membrane binding is mostly governed by C<sub>2</sub>A domain interactions.

### 3.3. Multiple sensors for spontaneous release

Many neurons co-express a fast sensor (Syt-1, 2 or 9) together with a sensor for slower asynchronous release (Syt-7) and for spontaneous (AP)-independent release (Doc2a,b), together encoding the complex stimulus-responsiveness of synaptic secretion<sup>107–109</sup>. The fact that co-expressed sensors operate together becomes apparent upon deletion of the fast Ca<sup>2+</sup>-sensor, leaving the remaining component still Ca<sup>2+</sup>-sensitive<sup>110,111</sup> yet showing altered Ca<sup>2+</sup>-dependency. In many systems the loss of fast release is accompanied by increased asynchronous and spontaneous release<sup>110–116</sup>. Given the co-existence of these multiple Ca<sup>2+</sup> sensors in synapses and other secretory systems, it remains the question how these sensors interact together to give rise to the overall stimulus-secretion coupling properties of the secretory apparatus<sup>109</sup>.

#### The competition model

One model hypothesizes that several Ca<sup>2+</sup> sensors with different Ca<sup>2+</sup>/membrane binding affinity and kinetics compete for vesicular release. This scenario is commonly used to explain why the deletion of one Ca<sup>2+</sup> sensor causes changes the Ca<sup>2+</sup>-sensitivity and cooperativity of release (for review)<sup>107</sup>. The occupancy of partially assembled SNARE complexes could be the biochemical basis for such competitive activity of Ca<sup>2+</sup> sensors. Subcellular targeting of fast sensors could provide a competitive advantage due to local enrichment at these sites, for example encoded by the N-terminal domain of Syt-1 and additional interactions of its cytosolic part with N-, P/Q-, L-type Ca<sup>2+</sup> channels irrespective of the presence of Ca<sup>2+</sup><sup>117–119</sup>. This model provides a plausible explanation for the increase in the apparent Ca<sup>2+</sup> sensitivity and higher release probability at resting Ca<sup>2+</sup> concentrations in absence of Syt-1 where Doc2 is able to occupy vacant Syt-1 driven release site (Chapter 6, see Figure 1).

Null mutations in Doc2a/b induces a decrease in spontaneous release rate by 50-75% compared to wildtype neurons<sup>3,4</sup>. In chapter 4, we investigated the relation between Doc2b Ca<sup>2+</sup>-binding site mutants and spontaneous release regulation. We suggest that resting stochastic release parallels Doc2b's Ca<sup>2+</sup>-dependent membrane binding (Chapter 4, Figure 2, 3, 5). A recent investigation revealed that removal of Doc2a/b in Syt-1 KO hippocampal neuron culture did not reduce the high mEPSCs rate, meaning that Doc2 proteins do not account for the increased minis upon Syt-1 ablation<sup>120</sup>. This outcome is supported by a prior publication<sup>4</sup> where they used an shRNA-dependent quadruple knockdown (KD) of all four



Ca<sup>2+</sup>-binding proteins of the Doc2 family in cortical neurons. Knockdown synapses exhibited a marked decrease in the spontaneous event frequency in Syt-1-expressing neurons, but the knockdown did not suppress the high spontaneous release frequency in Syt-1-deficient neurons. The remaining spontaneous release in Syt-1, Doc2a,b deficient neurons could be supported by a still undiscovered other class of Ca<sup>2+</sup>-sensor. In Chapter 5, we investigated several candidate C<sub>2</sub> domains proteins but did not identify the one responsible for the residual spontaneous release.

In addition to Syt-1 and Doc2, the high affinity Ca<sup>2+</sup>-sensor Syt-7 was shown to modulate the spontaneous component<sup>74,108</sup>. Electrophysiological investigations revealed no phenotype upon Syt-7 ablation in wildtype neurons<sup>121</sup> but its overexpression in Syt-1 KO neurons<sup>74</sup> and removal in Syt-2 KO neurons<sup>108</sup> respectively decreased and increased spontaneous exocytosis. Comparably to Syt-1, this suggests a supplementary clamping function for this isoform in absence of the fast sensor. This is not in line with evidence presented in chapter 5, as Syt-7 ablation in Doc2a, b, c, Raphilin knock-out genetic background had no effect on spontaneous release rate (Chapter 5, Figure 6), confirming that the effect of Syt-7 on this component only becomes apparent upon Syt-1, -2 removal. This hypothesis is supported by the fact that fast Ca<sup>2+</sup> sensors mask the role of Syt-7 in short-term plasticity<sup>122</sup> and asynchronous release<sup>108</sup>. Thus, a pattern is emerging where faster Ca<sup>2+</sup> sensors contribute more dominantly to overall synaptic release, masking the activities of the slower ones.

### The dual fusion / clamping model

An alternative explanation for the mixed effects of Syt-1/2 deletion on different phases of release states that fast sensors synchronize Ca<sup>2+</sup>-evoked release by a dual mechanism, which combines a positive role in fusion enhancement with an inhibitory role under resting conditions. This inhibitory role is often referred to as 'clamping'. Clamping could result from competitive inhibition of a more sensitive 2<sup>nd</sup> sensor as predicted by the competition model. Paradoxically, Syt-1 point mutations that moderately (D238N) or severely (R233Q) alter the apparent Ca<sup>2+</sup>-affinity for phospholipid binding decrease spontaneous release<sup>114</sup>. If clamping was mediated by the Ca<sup>2+</sup>-dependent membrane binding capacity of Syt-1, those mutations would have unclamped Doc2 (or other sensors) and increase spontaneous release. Instead, spontaneous release is reduced, meaning that spontaneous fusion inhibition isn't mediated by a membrane attachment mechanism.

A mutational analysis of Syt-2 identified a role of the poly-lysine motif in the C<sub>2</sub>B domain in spontaneous release inhibition<sup>111</sup>. In this study, the triple substitution K327Q, K328Q, K332Q blocked t-SNARE binding. The resulting Syt-2<sup>3K</sup> mutant fully rescued evoked release but lost its activity to inhibit spontaneous release at rest, demonstrating that clamping requires association with t-SNAREs or PIP<sub>2</sub>. In Syt-1, the clamping function was selectively affected in a variant termed Syt-1<sup>9Pro</sup>, in which proline substitutions in the flexible linker between C<sub>2</sub>A and C<sub>2</sub>B constrains the orientation of both domains relative to each other<sup>123</sup>. These observations suggest that the inhibitory mechanism is distinct from the fusogenic one, with differences pertaining to the relative disposition of the C<sub>2</sub> domains and the mode of target membrane association via t-SNAREs or PIP<sub>2</sub>.



The dual effect of Syt-1 is paralleled by complexins which clamp spontaneous release at rest by arresting SNARE complex zippering via its central helix and an accessory helical domain<sup>124,125</sup>. This  $\text{Ca}^{2+}$ -sensitive inhibition synchronizes  $\text{Ca}^{2+}$  triggered SVs fusion<sup>126</sup>. The collaborative action of Syt-1 and complexins in synchronizing  $\text{Ca}^{2+}$ -triggered membrane fusion is reinforced by a reconstituted single vesicle-vesicle fusion assay where Syt-1 and complexins individually inhibit spontaneous fusion and show a further negative effect when both incorporated<sup>126</sup>. A recent crystal structure of the SNARE proteins together with complexins and Syt-1 provides a structural basis for their synergistic function<sup>127</sup>. Altogether, this structure seems to constitute the elementary  $\text{Ca}^{2+}$ -sensitive platform in the primed vesicle state.

Díez-Arazola et al. reported an unexpected inhibitory effect of Doc2b on spontaneous release upon its overexpression in Syt-1, Doc2a,b TKO hippocampal neurons<sup>120</sup>. A plausible explanation is that this inhibition is caused by increased spontaneous GABA release in mixed cultures. Long-term spontaneous release of GABA can regulate the mEPSC frequency of glutamatergic cells in a mixed culture<sup>128</sup>. In addition, Doc2b is predominantly expressed in GABAergic neurons<sup>56</sup>. Thus, the inhibitory effect of Doc2b in excitatory neurons may be the consequence of an increased spontaneous GABA release specifically. This idea is consistent with the positive endogenous role of Doc2b in spontaneous release<sup>3</sup>. In chapter 4, neither Doc2 overexpression in wild type neurons (Chapter 4, Figure S3) nor its rescue in Doc2a,b KO neurons (Chapter 4, Figure 5) lower the mEPSC rate, indicating that endogenous Doc2b isn't limiting spontaneous release rate.

### 3.4. Working model: how Doc2 proteins drive spontaneous release

Fast  $\text{Ca}^{2+}$  sensors prevent spontaneous fusion at rest. This helps to preserve fusogenic vesicles for rapid fusion upon  $\text{Ca}^{2+}$  activation. The spontaneous component is strongly affected by the presence or absence of different Syts<sup>129,130</sup>. This property is likely to arise from the privileged location of Syts on the vesicle membrane (Syt-1) or the opposed PM (Syt-7). At rest the soluble Doc2 protein is localized in the cytosol (Chapter 6, Figure 1B) but can be recruited into the vicinity of fusion competent vesicles by various actors. The high  $\text{Ca}^{2+}$ -sensitivity and phospholipid affinity offer a near-resting activation capacity that is highly responsive to spontaneous  $\text{Ca}^{2+}$  fluctuations (Chapter 6, Figure 1C) or residual  $[\text{Ca}^{2+}]_i$  increases induced by synaptic activity. These  $\text{Ca}^{2+}$  fluctuations are too small to activate synaptotagmins (Chapter 6, see Figure 1D). This hypothesis is supported by previous finding where Doc2b dependent quantal release rate is strongly increased following train stimulation and extracellular  $\text{Ca}^{2+}$  rise<sup>3</sup> both of which conditions increase intracellular  $\text{Ca}^{2+}$  events (Chapter 3, Figure 4 and 6). Our model conceptualizes mechanisms of action of Doc2 in four different contexts (Chapter 6, Figure 1). During AP-dependent release, VGCC opening induces a spatially restrained  $\text{Ca}^{2+}$ -influx with a high peak concentration (Chapter 6, Figure 1A). In that scenario, Doc2 is mainly inactive in the cytoplasm. Few Doc2 copies might be present at the PM, by chance or recruited to it by a Munc13-, Munc18- or SNARE-dependent mechanisms. Synchronous neurotransmission is triggered by Syt-1 activation, located at the release site.

Syt-1 may inhibit Doc2 or Syt-7, competitively by release site occupancy (e.g steric hindrance at the primed proteolipid complex) or by active clamping together with complexins. In absence of AP depolarization, represented by the second scenario, spontaneous release is hypothetically driven by fast  $\text{Ca}^{2+}$  transients (SCTs) of short duration caused by activation of metabotropic receptors or VGCC flickering (Chapter 6, Figure 1B). Doc2 membrane association is determined by the basal resting  $[\text{Ca}^{2+}]_i$  and complementary recruitment pathways (Munc13, -18, SNAREs). In this context, spontaneous release may be triggered by Syt-1 or Doc2, depending on  $\text{Ca}^{2+}$  amplitude and the proximity of the sensors from the VGCC. This theory might be more relevant for GABAergic neurons because Syt-1 and Doc2b are both required for spontaneous release in inhibitory neurons<sup>56</sup>. The third scenario postulates that spontaneous release might be triggered by complex  $\text{Ca}^{2+}$  events (SCEs) generated by activation of metabotropic receptors or single or several VGCCs, amplified by the CICR process (Chapter 6, Figure 1C). The  $\text{Ca}^{2+}$  wave could enable a significant  $\text{Ca}^{2+}$ /Munc13-dependent Doc2 translocation and concomitantly induce Doc2-driven spontaneous release. In the fourth scenario, spontaneous events are generated by a global  $\text{Ca}^{2+}$  (Chapter 6, Figure 1D), as after a repetitive synaptic activity where residual  $\text{Ca}^{2+}$  gradually decreases. Syt-1 and Syt-7 are then inactive, but Doc2 could translocate to the PM and elicit spontaneous release. Massive activation of Doc2 could override the inhibitory effect of Syt-1 or alternatively, disassembly of Syt-1 oligomers after repeated synchronous release could enable Doc2 mediated fusion. Global  $[\text{Ca}^{2+}]_i$  could enable Doc2 translocation via simple  $\text{Ca}^{2+}$ -association or via DAG-dependent Munc13 binding.

In Chapter 4, we confirmed previously reported data on high  $\text{Ca}^{2+}$ -affinity properties of wildtype Doc2b (Chapter 4, Figure 3) but also showed a novel inhibitory effect of high  $[\text{Ca}^{2+}]$  on lipid binding behavior. At high  $\text{Ca}^{2+}$  concentration, the  $\text{C}_2\text{A}$  and  $\text{C}_2\text{AB}$  fragments (Chapter 4, Figure 3) showed a decreased liposome binding, suggesting that each sensor might only function in a limited  $[\text{Ca}^{2+}]$  window and are inhibited by higher  $[\text{Ca}^{2+}]$ . A striking parallel was observed between the  $\text{Ca}^{2+}$ -dependent lipid binding properties of Doc2b and its effect on exocytosis at rest or during activity (Chapter 4, Figure 5). Finally, we revealed a potential function in synaptic recovery (Chapter 4, Figure 7) which is likely regulated by residual  $\text{Ca}^{2+}$ , because the effect was abrogated in mutant forms. The "site-occupancy" model mentioned above fits well with our experimental results. Altogether, multiple  $\text{Ca}^{2+}$  sensors seem to be organized in hierarchy, dominated by Syt-1 (2 and 9; fast Syt) mediating the synchronous phase, followed by Syt-7 (slow Syt) involved in asynchronous release and finally Doc2 for spontaneous fusion. This hierarchy is likely based on their respective localization relative to the release machinery and their biophysical activation properties<sup>131</sup>.

### 3.5. Spontaneous release: $\text{Ca}^{2+}$ sensor or not?

An ongoing point of debate was whether Doc2b acts as a direct  $\text{Ca}^{2+}$ -sensitive protein for exocytosis<sup>3</sup> or as a structural element<sup>4</sup> (see chapter 4). Neutralization of two critical aspartates D218 and D220 in the  $\text{C}_2\text{A}$  domain of Doc2b appeared to mimic a  $\text{Ca}^{2+}$ -bound state which caused constitutive membrane enrichment<sup>2,105</sup> associated with an increased spontaneous release frequency<sup>3</sup> supporting its role as a  $\text{Ca}^{2+}$ -sensor<sup>3,47</sup>.

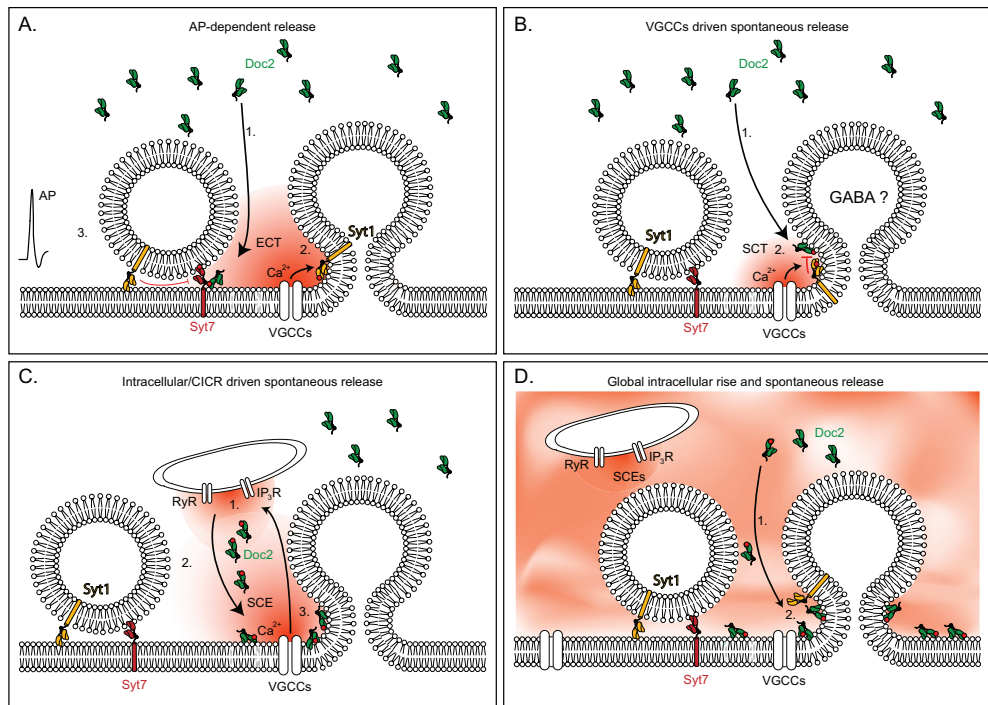


**Figure 1: Model for the interplay of  $\text{Ca}^{2+}$  sensors and the  $\text{Ca}^{2+}$ -sources which may trigger evoked (A) and spontaneous (B-D) release.** A. In the scenario of neuronal activity, VGCC opening induces a spatially restrained  $\text{Ca}^{2+}$ -influx with a high peak concentration. 1. Prior to the evoked  $\text{Ca}^{2+}$  transient, only few Doc2 copies might be recruited to the PM by a Munc13-, Munc18- or SNARE-dependent mechanism (these proteins are not depicted for simplicity). 2. Synchronous release is elicited by Syt-1 activation following the ECT. The  $\text{Ca}^{2+}$ -sensor activation following  $\text{Ca}^{2+}$  association is represented by a red dot on the  $\text{C}_2$  domain. In parallel, due to the preferential location of Syt-1 to the release site, its occupancy or sterical hindrance at the fusogenic proteolipid complex, Syt-1 may competitively inhibit Doc2 or Syt-7 (red arrows). 3. In a second phase or further away from  $\text{Ca}^{2+}$  nanodomains, Syt-1 is not activated and inhibits fusion, leaving the vesicle in a primed state where spontaneous fusion is unlikely. B. In the scenario of spontaneous release driven by VGCC flickering, fast SCTs occur which cause low-amplitude  $\text{Ca}^{2+}$  transients of short duration. 1. The proportion of membrane-bound Doc2 is determined by resting  $[\text{Ca}^{2+}]$ , and complementary recruitment pathways (Munc13, -18, SNAREs). 2. Spontaneous release may be triggered by Syt-1 or other sensors depending on  $\text{Ca}^{2+}$  amplitude, sensor affinity and proximity. This theory might be more relevant for GABAergic neurons because Syt-1 and Doc2b are both required for spontaneous release in inhibitory neurons, while Syt-1 is not necessary for mEPSCs which solely depend on Doc2a<sup>56</sup>. C. In the scenario of spontaneous release elicited by SCEs,  $\text{Ca}^{2+}$ -influx through single or several VGCCs could be amplified by RyR/IP<sub>3</sub>R opening (1.) (CICR). 2. This  $\text{Ca}^{2+}$  fluctuation would enable a significant  $\text{Ca}^{2+}$ /Munc13-dependent Doc2 translocation and concomitantly induce a (3.) SCE-dependent Doc2-driven spontaneous fusion event. D. In the last scenario of a global  $\text{Ca}^{2+}$  wave e.g. following a stimulation train, Syt-1 and Syt-7 are inactivated but Doc2 translocates to the PM (1.) and elicits spontaneous release. Under these conditions, massive activation of Doc2 could override the inhibitory effect of Syt-1 (2.). Moreover, global  $[\text{Ca}^{2+}]$  could enable Doc2 recruitment via simple  $\text{Ca}^{2+}$ -association but also via DAG-dependent Munc13 binding. In this state, VGCCs are closed but RyR and IP<sub>3</sub>R opening could nourish/maintain the  $\text{Ca}^{2+}$  wave.

Another  $\text{Ca}^{2+}$ -ligand mutant Doc2b<sup>6A</sup>, in which six critical aspartates were neutralized by alanine substitution, still supported spontaneous fusion while it did not bind  $\text{Ca}^{2+}$ , supporting its involvement as a structural element<sup>4</sup>. In chapter 4, we addressed the apparent discrepancy of those results and revealed that both mutants share very similar characteristics. Recently the 6A substitution was clearly identified as mimicking a  $\text{Ca}^{2+}$ -bound state<sup>56</sup>. In this experiment set, the mutant caused an increased mIPSC frequency that was largely  $\text{Ca}^{2+}$ -independent. These data, in agreement with the absence of translocation behavior and the  $\text{Ca}^{2+}$ -insensitive membrane binding properties consistently point to a  $\text{Ca}^{2+}$ -mimicking effect, causing gain-of-function behavior at rest. Recently, a genuine loss-of-function substitution was identified (D303N) which completely abolishes Doc2b translocation behavior<sup>2,56</sup> and its capacity to support asynchronous<sup>2</sup> or spontaneous release<sup>56</sup>. That draws a clear correlation between Doc2b  $\text{Ca}^{2+}$ -dependent membrane association and its ability to enhance exocytosis. The loss-of-function mutant is particularly interesting as it can be used as a negative control and provide clarification on Doc2b's function in exocytosis. Finally, the finding that the C<sub>2</sub>AB domain of Doc2b enhances hemifusion in a  $\text{Ca}^{2+}$ -dependent manner<sup>132,133</sup> further consolidates the  $\text{Ca}^{2+}$ -sensor theory.

Intracellular  $\text{Ca}^{2+}$ -chelation by BAPTA-AM provokes the loss of most (75% to >95%) spontaneous release events<sup>3,111,114</sup> and  $[\text{Ca}^{2+}]_e$  rise increases them<sup>3,4,114</sup> (Chapter 3, Figure 4 & 6). The  $\text{Ca}^{2+}$ -dependence could possibly reflect a pool recruitment mechanism. Vesicle recruitment is  $\text{Ca}^{2+}$ -dependent<sup>134</sup>. It accelerates during accumulation of  $\text{Ca}^{2+}$  within the presynaptic terminal<sup>135</sup> and diminishes after application of the fast  $\text{Ca}^{2+}$  buffer BAPTA, but not the slower buffer EGTA<sup>136</sup>. The process possibly involves synapsins, Munc13 alone or together with calmodulin<sup>137–139</sup>. In line with the positive effect of  $[\text{Ca}^{2+}]_e$  on global  $[\text{Ca}^{2+}]_i$  (Chapter 3, Figure 4A-C) and considering the effect of  $[\text{Ca}^{2+}]_i$  rise on the RRP size, the dependence of spontaneous release to extracellular  $\text{Ca}^{2+}$  might partially depend on the accumulation of release-ready vesicles, independently of  $\text{Ca}^{2+}$  sensors. The enhancement of synaptic recovery by Doc2b overexpression after train stimulations (Chapter 4, Figure 7) could imply a  $\text{Ca}^{2+}$ -sensitive function for Doc2b in RRP maintenance. Yet, no change in RRP size was found in Doc2 deficient neurons<sup>3,4</sup>. An evaluation of the RRP size by sucrose application upon various  $[\text{Ca}^{2+}]_e$  perfusion in either Doc2 removal or overexpression would clarify our questioning whether Doc2 speeds-up RRP refilling in a  $\text{Ca}^{2+}$ -dependent manner.

Another question is whether spontaneous release absolutely requires  $\text{Ca}^{2+}$  sensors or can be sensor-less, only needing SNARE zippering for spontaneous fusion of synaptic vesicles. Residual spontaneous events remain upon  $\text{Ca}^{2+}$ -chelation by EGTA and BAPTA<sup>3,34,37,111,114</sup>. This might be explained by the inability of the  $\text{Ca}^{2+}$ -chelators to completely absorb free  $\text{Ca}^{2+}$  ions, as the K<sub>d</sub> for EGTA and BAPTA is ~100 nM and spontaneous release could occur by  $[\text{Ca}^{2+}]_i$  below this value. Alternatively, a portion of spontaneous release could be  $\text{Ca}^{2+}$ -independent. *In vitro* reconstitution experiments with synaptobrevin and syntaxin-1–SNAP-25 incorporated into separate populations of liposomes<sup>140</sup> indicated that the SNAREs alone can induce vesicle fusion<sup>141</sup>. However, spontaneous events *in vivo* are tightly regulated and rendered  $\text{Ca}^{2+}$ -dependent by the complexin-Syt-SNARE complex, preventing stochastic fusion.

Still, one can imagine that a temporary lack of a strong fusion clamp would allow spontaneous SV fusion with the PM. Syt-1 was recently reported to self-assemble into a ring-like oligomers<sup>142</sup> which would be essential for the clamping function of Syt-1<sup>143</sup>. The latter investigation showed that destabilization of ring-shaped Syt-1 oligomers releases its clamping function, resulting in uncontrolled spontaneous fusion in absence of  $\text{Ca}^{2+}$ <sup>144</sup>. In this context, SVs would diffuse freely on the bilayer until they fuse spontaneously even in absence of  $\text{Ca}^{2+}$  sensors. This hypothesis provides an explanation for the spontaneous release phenotype in Syt-1 KO neurons and supports  $\text{Ca}^{2+}$ -independent spontaneous release.

### 3.5.1. The impact of mutation in $\text{C}_2$ domains

$\text{C}_2$  domains are centrally involved in  $\text{Ca}^{2+}$ -sensor function by interacting with SNAREs and membranes and they enhance membrane fusion (for review)<sup>145,146</sup>. Selective mutagenesis of the polybasic motif inhibited the SNARE interaction in Doc2b<sup>K237,319E</sup><sup>3</sup>, but did not abrogate liposome binding. Vice versa, substitution of the conserved amino acids H158, F222 and I360 to alanine in the  $\text{Ca}^{2+}$ -binding loops termed 4A mutation produced a lipid-binding-incompetent protein without blocking the SNARE interaction<sup>3</sup>. Thus, SNARE versus phospholipid association can happen independently. In chapter 4, we compared Doc2b<sup>DN</sup> and Doc2b<sup>6A</sup> mutations. Both versions of Doc2b mimic a  $\text{Ca}^{2+}$ -bound state (constitutively active) which enhance spontaneous release. The  $\text{Ca}^{2+}$  ligand site mutation D218,220,357,359N, termed C2A<sub>CLM</sub>B<sub>CLM</sub><sup>2,104</sup> abolishes  $\text{Ca}^{2+}$  association to  $\text{C}_2$  domains but greatly increases spontaneous fusion rate. Extensive mutagenesis work on Doc2b where the five critical aspartate residues in each  $\text{Ca}^{2+}$ -binding loop were mutated by paired or single substitutions showed that the D220N substitution within the  $\text{C}_2\text{A}$   $\text{Ca}^{2+}$ -binding-pocket is solely responsible for the constitutive membrane binding<sup>2</sup> and the mEPSC frequency increase. The behavior of the DN, 6A and CLM/CLM substitution is therefore explained by the single D220 neutralization which thus governs Doc2b lipid binding.

### 3.6. Distinct spontaneous release mechanisms in excitatory and inhibitory neurons

It was suggested that glutamatergic and GABAergic events are driven by the expression of Doc2a and -b respectively, although both isoforms are redundant in their ability to rescue spontaneous release<sup>56</sup>. In this study, both Syt-1 and Doc2 were confirmed to regulate minis. The contribution of Doc2a vs Doc2b on minis depends on whether one are dealing with glutamate or GABA secretion<sup>56</sup>. Single cell mRNA levels did not systematically corroborate specific expressions of Doc2a and Doc2b in pyramidal cells and interneurons respectively<sup>147</sup>. Yet, recent studies reported a predominant expression of Doc2a in CA3 pyramidal cells and of Doc2b in GABAergic striatum neurons<sup>56,148</sup>. The specific expression and function of Doc2a and b in excitatory and inhibitory neurons is still debated. It appears that mechanisms for  $\text{Ca}^{2+}$  signal that trigger spontaneous release at inhibitory but not excitatory synapses mostly rely on VGCCs<sup>33</sup>. Divergent outcomes were reported about the effect of  $[\text{Ca}^{2+}]_e$  on mEPSCs<sup>5</sup>. In our experiments (Chapter 3 and 5), the mEPSC frequency release rate correlated with global  $[\text{Ca}^{2+}]_i$  changes but the events were not time-locked to SCTs. This result from excitatory neurons does not exclude such coupling in GABAergic synapses (Chapter 3). It would thus be valuable to extend our investigation on the correlation between SCEs and spontaneous release to inhibitory neurons.

The high spontaneous release frequency in neurons lacking Syt-1 is more apparent in mixed glutamatergic/GABAergic pairs than in autaptic culture<sup>112,128</sup>. This is apparently the consequence of the GABAergic innervation of glutamatergic neurons. We can relate this finding to results we obtained in chapter 5 (Chapter 5, Figure 4) where spontaneous release increased upon rabphilin ablation in neuronal networks, but not autapses. Rabphilin might specifically promote spontaneous events in inhibitory neurons. Its ablation would then lower stochastic GABA release rates, indirectly causing a mEPSC frequency rise in networks. In light of all those findings, it can be recommended that investigations evaluating the implication of fusogenic proteins in spontaneous release take place in mixed glutamatergic/GABAergic cultures.

### 3.8. Candidate sensors: how to find them

Although our findings revealed no effect in favour of the regulation of minis by Doc2c, Syt-7 or rabphilin, many unidentified  $\text{Ca}^{2+}$  sensors could exist. Proteins containing  $\text{C}_2$  domains are potential candidates. Among the plethora of presynaptic proteins, Syt isoforms, Munc13s, ferlins and copines<sup>149</sup> are potential regulators of spontaneous fusion in glutamatergic hippocampal neurons. A  $\text{Ca}^{2+}$  sensor promoting spontaneous vesicle fusion is expected to meet several requirements. It should be active near resting  $\text{Ca}^{2+}$  concentrations and increase the release probability of fusion in the absence of the fast sensors Syt-1, -2<sup>109,110</sup>. It should display high  $\text{Ca}^{2+}$ -sensitivity of membrane binding, higher than Syt-1 and Syt-7 and be present at least temporarily in the vicinity of fusion competent vesicles. Additional bioinformatics analysis, based on sequence profile searches, phylogenetic and phyletic-pattern and structure-prediction, have implemented the long list of proteins containing  $\text{C}_2$  domains and greatly facilitate the quest. Related  $\text{C}_2$  domain proteins have been included in the large collection of proteins families of the PFAM database (<http://pfam.sanger.ac.uk>). Proteins showing a high degree of amino acid sequence homology with Syts and Doc2s should then be favoured.

## 4. Spontaneous release in health and pathologies

Miniature synaptic potentials have been considered for long as physiologically meaningless events and only considered to define the size of a quantum, quantal release evoked by an AP and modeling of random release<sup>150</sup>. Yet, consideration towards spontaneous release changed as cortical and hippocampal neurons were shown to sometimes communicate via a single synapse which release only one neurotransmitter quantum (mini) upon minimal stimulation<sup>151–153</sup>. It suggests that single quantum release must have a physiological importance. Interest in spontaneous release grew further as investigations exposed that spontaneous release can produce a significant inhibitory tone in postsynaptic neurons<sup>154</sup> and influence the firing of small interneurons<sup>155</sup>. It can then directly shape neuronal excitability as inhibitory quanta could rapidly terminate neuronal firing whereas small numbers of coincident excitatory quanta can trigger firing<sup>155</sup>. Alternatively, spontaneous release modulates postsynaptic excitability by regulating the tonic activity of high-affinity receptors<sup>154,156</sup>. Low concentrations of ambient GABA can persistently activate certain synaptic and extrasynaptic GABA receptors to generate a tonic conductance.



Spontaneous release also participates in postsynaptic homeostasis in mature synapses. Synaptic homeostasis is a process based on feedback regulation which enables the tuning of neurotransmission efficiency to maintain neuron excitability balance. It was suggested to be independent of evoked neurotransmission at the *Drosophila* NMJ<sup>157</sup> as it appeared in presence of TTX. An increase in evoked synaptic strength, resulting from an increase in the efficacy of transmission was reported after blockade of postsynaptic receptors for several minutes. The mechanism implicated presynaptic modulation of VGCCs ( $\text{CaV}_{2.1}$ ) by retrograde signaling. AP-independent homeostatic plasticity could be partially regulated by minis. Synaptic scaling can be engaged by a change in AMPA receptor density. Initial experiments in *in vitro* models revealed that pharmacological blockade of activity (TTX) scales up the AMPA-receptor mediated mEPSCs amplitude<sup>158</sup>. The effect of spontaneous neurotransmitter release on synaptic structure conservation and postsynaptic scaling is likely mediated by the immobilization and density maintenance of postsynaptic receptors<sup>159–161</sup>.

Spontaneous release may also play a role during development. It was suggested to modulate postsynaptic enzymatic activity and protein synthesis<sup>162,163</sup>. Minis might keep resting protein synthesis processes in check and sensitive to stimuli for synapse strengthening. Rat hippocampal neurons show very high levels of exclusively spontaneous release in young neurons, which progressively decrease during synapse formation and maturation<sup>164</sup>. Cortical layer 4 neurons also display an important increase in spontaneous events from development stages P12 to P23<sup>165</sup>. Neurotransmitters are released spontaneously from the growth cones of embryonic neurons<sup>166</sup>, suggesting a role in nerve growth and axon guidance. One model proposes that spontaneous glutamate release from developing axons organizes axodendritic contact by signaling over long ranges to NMDA receptors on developing dendrites<sup>167</sup>, thereby shaping neuronal arborization. Once synaptic contact is established, postsynaptic protein synthesis required for continued growth cone guidance is stopped<sup>163,168</sup>. Therefore, spontaneous release of neurotransmitter might be important in the wiring of the brain during development<sup>169</sup>. Spontaneous release is also involved in the maintenance of dendritic spines via AMPAR receptor activation<sup>170</sup>. CA1 pyramidal cell spines decreased in density and length after application of an AMPAR antagonist but not TTX, suggesting that spontaneous input is sufficient for synaptic maintenance.

Precise control of synaptic development, connectivity and maintenance is critical for brain functions. The function of spontaneous release detailed above raises the question which neuropathologies may be triggered in case of dysregulation. One can easily imagine that aberrant development of neuronal circuitry could lead to drug-resistant epilepsy<sup>171,172</sup>, encephalopathy or autism where mEPSC increases in a critical time window were correlated to the risk of Autism Spectrum Disorders<sup>173</sup>. Disorders associated with faulty neuronal circuits also include schizophrenia<sup>174</sup> or fragile X Syndrome<sup>175</sup>. This is corroborated by findings that point to an increased expression of DOC2A (involved in spontaneous release regulation) has been observed in human and rat models of Temporal Lobe Epilepsy<sup>176</sup>, while copy number variants of DOC2A have been associated with Schizophrenia<sup>177</sup>.

## 5. Conclusion, perspectives and future directions

The work described in this thesis explored neurotransmitter release regulation by spontaneous presynaptic  $\text{Ca}^{2+}$  fluctuations and several  $\text{C}_2$  domain proteins at excitatory hippocampal synapses. Prior studies have revealed the complexity of the  $\text{Ca}^{2+}$ -dependent neurotransmitter release in neurons. Despite the physiological significance of spontaneous release, a direct evidence for a relationship between cytosolic  $\text{Ca}^{2+}$ -signals and resting vesicle fusion is still missing. The first part of this thesis examined presynaptic SCEs and SCTs. The SICT method developed for  $\text{Ca}^{2+}$ -imaging data analysis significantly accelerated the analysis and appeared sensitive enough to detect changes in the spontaneous release frequency induced by caffeine.  $[\text{Ca}^{2+}]_c$  increased both bulk/global cytosolic  $[\text{Ca}^{2+}]$  and SCEs in parallel with the mEPSC frequency rise. Although increases in  $[\text{Ca}^{2+}]_c$  clearly enhanced minis, a tight coupling between SCEs and mEPSCs was not detected. Calcium transients triggered by intracellular  $\text{Ca}^{2+}$  sources typically give rise to slower  $\text{Ca}^{2+}$  waveforms. Additional studies are necessary to further unravel the  $\text{Ca}^{2+}$ -dependency of spontaneous neurotransmission. New optical tools, such as syHyJREx are good opportunities to investigate any temporal relation between  $\text{Ca}^{2+}$  and spontaneous SV fusion. Using this dual indicator, efforts should be made to evaluate the role of different  $\text{Ca}^{2+}$  influx pathways by examining a temporal coupling at high  $\text{Ca}^{2+}$ , upon  $\text{Cd}^{2+}$  blockade of VGCCs, in presence of selective VGCC blockers ( $\omega$ -Agatoxin for P/Q-type channels;  $\omega$ -Conotoxin for N-type; SNX-482 for R-type and TTA-P2 for T-type channels) <sup>5</sup> in parallel with  $\text{Ca}^{2+}$ -store depletion by thapsigargin both in glutamatergic and GABAergic neurons. Additional insight could be gained by the development and use of  $\text{Ca}^{2+}$  probes offering higher  $\text{Ca}^{2+}$  detection sensitivity and speed (or faster  $\text{Ca}^{2+}$  association). Altogether, extensive studies of the different types of  $\text{Ca}^{2+}$  events and their sources are necessary to apprehend their physiological role.

The second part of this thesis focused on the regulation of evoked and spontaneous neurotransmitter release by various  $\text{C}_2$  domain proteins. We established that two Doc2b mutants, Doc2b<sup>DN</sup> and <sup>6A</sup> previously categorized respectively as gain and loss of function both constitutively bind to the plasma membrane. The modification of Doc2b  $\text{Ca}^{2+}$ -dependent properties altered spontaneous release rate, supporting its role as a  $\text{Ca}^{2+}$  sensor in the release process. Furthermore, potential other  $\text{Ca}^{2+}$  sensors were investigated regarding their regulation of residual spontaneous release in absence of Doc2a,b. Rabphilin ablation altered mEPSC frequency selectively in neuronal networks, suggesting a positive role on quantal GABA release. Yet, no apparent effect on spontaneous release became prominent upon removal of Doc2c or Syt-7.

Additional investigations are necessary to definitely determine the function of the above-mentioned proteins in spontaneous fusion. Because fast sensors can mask the effects of slower ones, one suggestion would be to examine the effect of Rabphilin, Doc2c and Syt-7 deletion in absence of Syt-1 in excitatory and inhibitory neurons.

Overall, the findings presented in this thesis provide new insight on the regulation of quantal release by  $\text{Ca}^{2+}$  signaling and  $\text{C}_2$  proteins. Despite a collective effort made to decipher the



regulation of spontaneous neurotransmission by multiple sensors, several questions remain: What are the molecular mechanisms and interactor molecules necessary for the inhibition of second sensors by fast sensors? Also, does this inhibitory activity require activation of fast sensors or is it a function that happens at rest? Is the dual capacity of Syt-1 to promote and clamp SVs fusion a common feature for all C<sub>2</sub> domains implicated in neurotransmission? Are the fine-tuned expression levels of fast sensors relative to other sensors important for the Ca<sup>2+</sup>-dependency of neurotransmitter release and short-term plasticity? Answers will considerably increase our knowledge of synaptic physiology, with essential implications for overall brain function.

## References

1. Yao, J., Gaffaney, J. D., Kwon, S. E. & Chapman, E. R. Doc2 is a  $\text{Ca}^{2+}$  sensor required for asynchronous neurotransmitter release. *Cell* 147, 666–77 (2011).
2. Xue, R., Gaffaney, J. D. & Chapman, E. R. Structural elements that underlie Doc2 $\beta$  function during asynchronous synaptic transmission. *Proc. Natl. Acad. Sci.* 112, 201502288 (2015).
3. Groffen, A. J. et al. Doc2b Is a High-Affinity  $\text{Ca}^{2+}$  Sensor for Spontaneous Neurotransmitter Release. *Science* (80-. ). 327, 1614–1618 (2010).
4. Pang, Z. P. et al. Doc2 supports spontaneous synaptic transmission by a  $\text{Ca}^{2+}$ -independent mechanism. *Neuron* 70, 244–51 (2011).
5. Ermolyuk, Y. S. et al. Differential triggering of spontaneous glutamate release by P/Q-, N- and R-type  $\text{Ca}^{2+}$  channels. *Nat. Neurosci.* 16, 1754–63 (2013).
6. Emptage, N. J., Reid, C. A. & Fine, A. Calcium stores in hippocampal synaptic boutons mediate short-term plasticity, store-operated  $\text{Ca}^{2+}$  entry, and spontaneous transmitter release. *Neuron* 29, 197–208 (2001).
7. Llano, I. et al. Presynaptic calcium stores underlie large-amplitude miniature IPSCs and spontaneous calcium transients. *Nat. Neurosci.* 3, 1256–1265 (2000).
8. Kiselyov, K., Shin, D. M. & Muallem, S. Signalling specificity in GPCR-dependent  $\text{Ca}^{2+}$  signalling. *Cell. Signal.* 15, 243–253 (2003).
9. Patel, T. P., Man, K., Firestein, B. L. & Meaney, D. F. Automated quantification of neuronal networks and single-cell calcium dynamics using calcium imaging. *J. Neurosci. Methods* 243, 26–38 (2015).
10. Prada, J. et al. An open source tool for automatic spatiotemporal assessment of calcium transients and local ‘signal-close-to-noise’ activity in calcium imaging data. *PLoS Comput. Biol.* 14, e1006054 (2018).
11. Quinlan, M. E., Alberto, C. O. & Hirasawa, M. Short-term potentiation of mEPSCs requires N-, P/Q- and L-type  $\text{Ca}^{2+}$  channels and mitochondria in the supraoptic nucleus. *J. Physiol.* 586, 3147–61 (2008).
12. Lefkowitz, J. J. et al. Suppression of  $\text{Ca}^{2+}$  syntillas increases spontaneous exocytosis in mouse adrenal chromaffin cells. *J. Gen. Physiol.* 134, 267–80 (2009).
13. De Crescenzo, V. et al.  $\text{Ca}^{2+}$  syntillas, miniature  $\text{Ca}^{2+}$  release events in terminals of hypothalamic neurons, are increased in frequency by depolarization in the absence of  $\text{Ca}^{2+}$  influx. *J. Neurosci.* 24, 1226–35 (2004).
14. Simon, S. M. & Llinás, R. R. Compartmentalization of the submembrane calcium activity during calcium influx and its significance in transmitter release. *Biophys. J.* 48, 485–98 (1985).
15. Augustine, G. J., Santamaria, F. & Tanaka, K. Local calcium signaling in neurons. *Neuron* 40, 331–346 (2003).
16. Berridge, M. J. Calcium microdomains: organization and function. *Cell Calcium* 40, 405–12 (2006).
17. Llinás, R., Steinberg, I. Z. & Walton, K. Relationship between presynaptic calcium current and postsynaptic potential in squid giant synapse. *Biophys. J.* 33, 323–51 (1981).
18. Katz, B. & Miledi, R. THE MEASUREMENT OF SYNAPTIC DELAY, AND THE TIME COURSE OF ACETYLCHOLINE RELEASE AT THE NEUROMUSCULAR JUNCTION. *Proc. R. Soc. London. Ser. B, Biol. Sci.* 161, 483–95 (1965).
19. Südhof, T. C. Calcium control of neurotransmitter release. *Cold Spring Harb. Perspect. Biol.* 4, a011353 (2012).
20. Katz, B. & Miledi, R. Ionic requirements of synaptic transmitter release. *Nature* 215, 651 (1967).
21. Südhof, T. C. Neurotransmitter release: the last millisecond in the life of a synaptic vesicle. *Neuron* 80, 675–90 (2013).
22. Sabatini, B. L. & Regehr, W. G. Timing of neurotransmission at fast synapses in the mammalian brain. *Nature* 384, 170–2 (1996).
23. Meinrenken, C. J., Borst, J. G. G. & Sakmann, B. Calcium secretion coupling at calyx of Held governed by nonuniform channel-vesicle topography. *J. Neurosci.* 22, 1648–67 (2002).
24. Meinrenken, C. J., Borst, J. G. G. & Sakmann, B. Local routes revisited: The space and time dependence of the  $\text{Ca}^{2+}$  signal for phasic transmitter release at the rat calyx of Held. *J. Physiol.* 547, 665–689 (2003).
25. Zhai, R. G. & Bellen, H. J. The Architecture of the Active Zone in the Presynaptic Nerve Terminal. *Physiology* 19, 262–270 (2004).
26. Stanley, E. F. The calcium channel and the organization of the presynaptic transmitter release face. *Trends Neurosci.* 20, 404–9 (1997).
27. Chen, T.-W. et al. Ultrasensitive fluorescent proteins for imaging neuronal activity. *Nature* 499, 295–300 (2013).
28. Nakai, J., Ohkura, M. & Imoto, K. A high signal-to-noise  $\text{Ca}^{2+}$  probe composed of a single green fluorescent protein. *Nat. Biotechnol.* 19, 137–141 (2001).
29. Nakamura, Y. et al. Nanoscale Distribution of Presynaptic  $\text{Ca}^{2+}$  Channels and Its Impact on Vesicular Release during Development. *Neuron* 85, 145–158 (2015).
30. Ghelani, T. & Sigrist, S. J. Coupling the Structural and Functional Assembly of Synaptic Release Sites. *Front.*

Neuroanat. 12, 81 (2018).

31. Bennett, M. R., Farnell, L. & Gibson, W. G. The probability of quantal secretion near a single calcium channel of an active zone. *Biophys. J.* 78, 2201–21 (2000).
32. Sharma, G. & Vijayaraghavan, S. Modulation of presynaptic store calcium induces release of glutamate and postsynaptic firing. *Neuron* 38, 929–39 (2003).
33. Williams, C. L. & Smith, S. M. Calcium dependence of spontaneous neurotransmitter release. *J. Neurosci. Res.* 96, 335–347 (2018).
34. Simkus, C. R. L. & Stricker, C. The contribution of intracellular calcium stores to mEPSCs recorded in layer II neurones of rat barrel cortex. *J. Physiol.* 545, 521–535 (2002).
35. Vyleta, N. P. & Smith, S. M. Spontaneous glutamate release is independent of calcium influx and tonically activated by the calcium-sensing receptor. *J. Neurosci.* 31, 4593–4606 (2011).
36. Reese, A. L. & Kavalali, E. T. Spontaneous neurotransmission signals through store-driven  $\text{Ca}(2+)$  transients to maintain synaptic homeostasis. *Elife* 4, 1–15 (2015).
37. Angleson, J. K. & Betz, W. J. Intraterminal  $\text{Ca}(2+)$  and spontaneous transmitter release at the frog neuromuscular junction. *J. Neurophysiol.* 85, 287–94 (2001).
38. Mulkey, R. M. & Zucker, R. S. Calcium released by photolysis of DM-nitrophen triggers transmitter release at the crayfish neuromuscular junction. *J. Physiol.* 462, 243–60 (1993).
39. Ravin, R., Spira, M. E., Parnas, H. & Parnas, I. Simultaneous measurement of intracellular  $\text{Ca}2+$  and asynchronous transmitter release from the same crayfish bouton. *J. Physiol.* 501 ( Pt 2, 251–62 (1997).
40. Helmchen, F., Borst, J. G. & Sakmann, B. Calcium dynamics associated with a single action potential in a CNS presynaptic terminal. *Biophys. J.* 72, 1458–71 (1997).
41. Maravall, M., Mainen, Z. F., Sabatini, B. L. & Svoboda, K. Estimating intracellular calcium concentrations and buffering without wavelength ratioing. *Biophys. J.* 78, 2655–2667 (2000).
42. Sabatini, B. L., Oertner, T. G. & Svoboda, K. The life cycle of  $\text{Ca}2+$  ions in dendritic spines. *Neuron* 33, 439–452 (2002).
43. Scott, R. & Rusakov, D. A. Main determinants of presynaptic  $\text{Ca}2+$  dynamics at individual mossy fiber-CA3 pyramidal cell synapses. *J. Neurosci* 26, 7071–7081 (2006).
44. Schneggenburger, R. & Neher, E. Intracellular calcium dependence of transmitter release rates at a fast central synapse. *Nature* 406, 889–93 (2000).
45. Lou, X., Scheuss, V. & Schneggenburger, R. Allosteric modulation of the presynaptic  $\text{Ca}2+$  sensor for vesicle fusion. *Nature* 435, 497–501 (2005).
46. Neher, E. & Sakaba, T. Multiple roles of calcium ions in the regulation of neurotransmitter release. *Neuron* 59, 861–72 (2008).
47. Groffen, A. J. A., Friedrich, R., Brian, E. C., Ashery, U. & Verhage, M. DOC2A and DOC2B are sensors for neuronal activity with unique calcium-dependent and kinetic properties. *J. Neurochem.* 97, 818–833 (2006).
48. Li, C. et al.  $\text{Ca}(2+)$ -dependent and -independent activities of neural and non-neural synaptotagmins. *Nature* 375, 594–9 (1995).
49. Radhakrishnan, A., Stein, A., Jahn, R. & Fasshauer, D. The  $\text{Ca}2+$  affinity of synaptotagmin 1 is markedly increased by a specific interaction of its C2B domain with phosphatidylinositol 4,5-bisphosphate. *J. Biol. Chem.* 284, 25749–60 (2009).
50. Orita, S. et al. Physical and functional interactions of Doc2 and Munc13 in  $\text{Ca}2+$ -dependent exocytotic machinery. *J. Biol. Chem.* 272, 16081–4 (1997).
51. Duncan, R. R., Betz, A., Shipston, M. J., Brose, N. & Chow, R. H. Transient, phorbol ester-induced DOC2-Munc13 interactions in vivo. *J. Biol. Chem.* 274, 27347–27350 (1999).
52. Friedrich, R., Gottfried, I. & Ashery, U. Munc13-1 translocates to the plasma membrane in a Doc2B- and calcium-dependent manner. *Front. Endocrinol. (Lausanne)*. 4, 1–6 (2013).
53. Xue, R. et al. Doc2-mediated superpriming supports synaptic augmentation. *Proc. Natl. Acad. Sci. U. S. A.* 115, E5605–E5613 (2018).
54. Verhage, M. et al. DOC2 proteins in rat brain: complementary distribution and proposed function as vesicular adapter proteins in early stages of secretion. *Neuron* 18, 453–61 (1997).
55. Ramalingam, L., Lu, J., Hudmon, A. & Thurmond, D. C. Doc2b serves as a scaffolding platform for concurrent binding of multiple Munc18 isoforms in pancreatic islet  $\beta$ -cells. *Biochem. J.* 464, 251–8 (2014).
56. Courtney, N. A., Briguglio, J. S., Bradberry, M. M., Greer, C. & Chapman, E. R. Excitatory and Inhibitory Neurons Utilize Different  $\text{Ca}2+$  Sensors and Sources to Regulate Spontaneous Release. *Neuron* 98, 977-991.e5 (2018).
57. Liu, H. et al. Spontaneous Vesicle Fusion Is Differentially Regulated at Cholinergic and GABAergic Synapses. *Cell Rep.* 22, 2334–2345 (2018).
58. Tsintsadze, T., Williams, C. L., Weingarten, D. J., von Gersdorff, H. & Smith, S. M. Distinct Actions of Voltage-

- Activated Ca<sup>2+</sup> Channel Block on Spontaneous Release at Excitatory and Inhibitory Central Synapses. *J. Neurosci.* 37, 4301–4310 (2017).
59. Miesenböck, G., De Angelis, D. A. & Rothman, J. E. Visualizing secretion and synaptic transmission with pH-sensitive green fluorescent proteins. *Nature* 394, 192–195 (1998).
60. Granseth, B., Odermatt, B., Royle, S. J. & Lagnado, L. Clathrin-Mediated Endocytosis Is the Dominant Mechanism of Vesicle Retrieval at Hippocampal Synapses. *Neuron* 51, 773–786 (2006).
61. Li, H. et al. Concurrent imaging of synaptic vesicle recycling and calcium dynamics. *Front. Mol. Neurosci.* 4, 34 (2011).
62. Li, Y. & Tsien, R. W. PHTomato, a red, genetically encoded indicator that enables multiplex interrogation of synaptic activity. *Nat. Neurosci.* 15, 1047–1053 (2012).
63. Zhao, Y. et al. An expanded palette of genetically encoded Ca<sup>2+</sup> indicators. *Science* 333, 1888–91 (2011).
64. Jackson, R. E. & Burrone, J. Visualizing Presynaptic Calcium Dynamics and Vesicle Fusion with a Single Genetically Encoded Reporter at Individual Synapses. *Front. Synaptic Neurosci.* 8, 21 (2016).
65. Wu, J. et al. A long Stokes shift red fluorescent Ca<sup>2+</sup> indicator protein for two-photon and ratiometric imaging. *Nat Commun* 5, 5262 (2014).
66. Klapoetke, N. C. et al. Independent optical excitation of distinct neural populations. *Nat. Methods* 11, 338–46 (2014).
67. Rizo, J. & Südhof, T. C. C2 domains, structure and function of a universal Ca<sup>2+</sup>-binding domain. *J. Biol. Chem.* 273, 15879–15882 (1998).
68. Gomperts, B. D., Kramer, Ij. M. & Tatham, P. E. R. Phosphorylation and Dephosphorylation: Protein Kinases A and C in *Signal Transduction* 243–272 (Elsevier, 2009). doi:10.1016/B978-0-12-369441-6.00009-X
69. Benes, C. H. et al. The C2 domain of PKC $\delta$  is a phosphotyrosine binding domain. *Cell* 121, 271–80 (2005).
70. Maximov, A., Shin, O.-H., Liu, X. & Südhof, T. C. Synaptotagmin-12, a synaptic vesicle phosphoprotein that modulates spontaneous neurotransmitter release. *J. Cell Biol.* 176, 113–24 (2007).
71. Fukuda, M. & Mikoshiba, K. Doc2 $\gamma$ , a Third Isoform of Double C2 Protein, Lacking Calcium-Dependent Phospholipid Binding Activity. *Biochem. Biophys. Res. Commun.* 276, 626–632 (2000).
72. Fukuda, M., Saegusa, C., Kanno, E. & Mikoshiba, K. The C2A Domain of Double C2 Protein  $\gamma$  Contains a Functional Nuclear Localization Signal. *J. Biol. Chem.* 276, 24441–24444 (2001).
73. Corbalan-García, S. & Gómez-Fernández, J. C. Signaling through C2 domains: more than one lipid target. *Biochim. Biophys. Acta* 1838, 1536–47 (2014).
74. Bacaj, T. et al. Synaptotagmin-1 and Synaptotagmin-7 Trigger Synchronous and Asynchronous Phases of Neurotransmitter Release. *Neuron* 80, 947–959 (2013).
75. Yue, F. et al. A comparative encyclopedia of DNA elements in the mouse genome. *Nature* 515, 355–64 (2014).
76. Ljubojevic, S. & Bers, D. M. Nuclear calcium in cardiac myocytes. *J. Cardiovasc. Pharmacol.* 65, 211–7 (2015).
77. Araç, D. et al. Close membrane-membrane proximity induced by Ca<sup>2+</sup>-dependent multivalent binding of synaptotagmin-1 to phospholipids. *Nat. Struct. Mol. Biol.* 13, 209–217 (2006).
78. Striegel, A. R. et al. Calcium binding by synaptotagmin's C2A domain is an essential element of the electrostatic switch that triggers synchronous synaptic transmission. *J. Neurosci.* 32, 1253–1260 (2012).
79. Shao, X. et al. Synaptotagmin–Syntaxin Interaction: The C2 Domain as a Ca<sup>2+</sup>-Dependent Electrostatic Switch. *Neuron* 18, 133–142 (1997).
80. Giladi, M. et al. The C2B domain is the primary Ca<sup>2+</sup> sensor in DOC2B: a structural and functional analysis. *J. Mol. Biol.* 425, 4629–4641 (2013).
81. García, J., Gerber, S. H., Sugita, S., Südhof, T. C. & Rizo, J. A conformational switch in the Piccolo C2A domain regulated by alternative splicing. *Nat. Struct. Mol. Biol.* 11, 45–53 (2004).
82. Gerber, S. H., García, J., Rizo, J. & Südhof, T. C. An unusual C(2)-domain in the active-zone protein piccolo: implications for Ca(2+) regulation of neurotransmitter release. *EMBO J.* 20, 1605–19 (2001).
83. Biadene, M., Montaville, P., Sheldrick, G. M. & Becker, S. Structure of the C2A domain of rabphilin-3A. *Acta Crystallogr. D. Biol. Crystallogr.* 62, 793–9 (2006).
84. Farah, C. A. & Sossin, W. S. The role of C2 domains in PKC signaling. *Adv Exp Med Biol* 740, 663–683 (2012).
85. Shin, O.-H., Xu, J., Rizo, J. & Südhof, T. C. Differential but convergent functions of Ca<sup>2+</sup> binding to synaptotagmin-1 C2 domains mediate neurotransmitter release. *Proc. Natl. Acad. Sci. U. S. A.* 106, 16469–16474 (2009).
86. Hui, E., Bai, J. & Chapman, E. R. Ca<sup>2+</sup>-triggered simultaneous membrane penetration of the tandem C2 domains of synaptotagmin I. *Biophys. J.* 91, 1767–77 (2006).
87. Martens, S., Kozlov, M. M. & McMahon, H. T. How synaptotagmin promotes membrane fusion. *Science* 316, 1205–8 (2007).
88. McMahon, H. T., Kozlov, M. M. & Martens, S. Membrane curvature in synaptic vesicle fusion and beyond. *Cell* 140, 601–5 (2010).

89. Hui, E., Johnson, C. P., Yao, J., Dunning, F. M. & Chapman, E. R. Synaptotagmin-mediated bending of the target membrane is a critical step in  $\text{Ca}^{2+}$ -regulated fusion. *Cell* 138, 709–21 (2009).
90. Connell, E. et al. Cross-linking of Phospholipid Membranes is a Conserved Property of Calcium-sensitive Synaptotagmins. *J. Mol. Biol.* 380, 42–50 (2008).
91. Herrick, D. Z., Sterbling, S., Rasch, K. A., Hinderliter, A. & Cafiso, D. S. Position of Synaptotagmin I at the Membrane Interface: Cooperative Interactions of Tandem C2 Domains †. *Biochemistry* 45, 9668–9674 (2006).
92. Tran, H. T., Anderson, L. H. & Knight, J. D. Membrane-Binding Cooperativity and Coinsertion by C2AB Tandem Domains of Synaptotagmins 1 and 7. *Biophys. J.* 116, 1025–1036 (2019).
93. Fernández-Chacón, R. et al. Structure/Function Analysis of  $\text{Ca}^{2+}$  Binding to the C2 A Domain of Synaptotagmin 1. *J. Neurosci.* 22, 8438–8446 (2002).
94. Mackler, J. M., Drummond, J. a, Loewen, C. a, Robinson, I. M. & Reist, N. E. The C(2)B  $\text{Ca}^{2+}$ -binding motif of synaptotagmin is required for synaptic transmission in vivo. *Nature* 418, 340–344 (2002).
95. Nishiki, T. -i. T. & Augustine, G. J. Dual Roles of the C2B Domain of Synaptotagmin I in Synchronizing  $\text{Ca}^{2+}$ -Dependent Neurotransmitter Release. *J. Neurosci.* 24, 8542–8550 (2004).
96. Bowers, M. R. & Reist, N. E. The C2A domain of synaptotagmin is an essential component of the calcium sensor for synaptic transmission. *PLoS One* 15, e028348 (2020).
97. Pang, Z. P., Shin, O.-H., Meyer, A. C., Rosenmund, C. & Südhof, T. C. A gain-of-function mutation in synaptotagmin-1 reveals a critical role of  $\text{Ca}^{2+}$ -dependent soluble N-ethylmaleimide-sensitive factor attachment protein receptor complex binding in synaptic exocytosis. *J. Neurosci.* 26, 12556–65 (2006).
98. Fernández-Chacón, R. et al. Synaptotagmin I functions as a calcium regulator of release probability. *Nature* 410, 41–49 (2001).
99. Zhang, X., Rizo, J. & Südhof, T. C. Mechanism of phospholipid binding by the C2A-domain of synaptotagmin I. *Biochemistry* 37, 12395–403 (1998).
100. Wang, P., Wang, C.-T., Bai, J., Jackson, M. B. & Chapman, E. R. Mutations in the effector binding loops in the C2A and C2B domains of synaptotagmin I disrupt exocytosis in a nonadditive manner. *J. Biol. Chem.* 278, 47030–7 (2003).
101. Brandt, D. S., Coffman, M. D., Falke, J. J. & Knight, J. D. Hydrophobic contributions to the membrane docking of synaptotagmin 7 C2A domain: mechanistic contrast between isoforms 1 and 7. *Biochemistry* 51, 7654–64 (2012).
102. Voleti, R., Tomchick, D. R., Südhof, T. C. & Rizo, J. Exceptionally tight membrane-binding may explain the key role of the synaptotagmin-7 C2A domain in asynchronous neurotransmitter release. *Proc. Natl. Acad. Sci. U. S. A.* 114, E8518–E8527 (2017).
103. Xue, M. et al. Structural and mutational analysis of functional differentiation between synaptotagmins-1 and -7. *PLoS One* 5, 1–12 (2010).
104. Gaffaney, J. D., Xue, R. & Chapman, E. R. Mutations that disrupt  $\text{Ca}^{2+}$ -binding activity endow Doc2 $\beta$  with novel functional properties during synaptic transmission. *Mol. Biol. Cell* 25, 481–494 (2014).
105. Friedrich, R. et al. DOC2B acts as a calcium switch and enhances vesicle fusion. *J. Neurosci.* 28, 6794–6806 (2008).
106. Bourgeois-Jaarsma, Q., Verhage, M. & Groffen, A. J. Doc2b  $\text{Ca}^{2+}$  binding site mutants enhance synaptic release at rest at the expense of sustained synaptic strength. *Sci. Rep.* 9, 14408 (2019).
107. Volynski, K. E. & Krishnakumar, S. S. Synergistic control of neurotransmitter release by different members of the synaptotagmin family. *Curr. Opin. Neurobiol.* 51, 154–162 (2018).
108. Luo, F. & Südhof, T. C. Synaptotagmin-7-Mediated Asynchronous Release Boosts High-Fidelity Synchronous Transmission at a Central Synapse. *Neuron* 94, 826–839.e3 (2017).
109. Walter, A. M., Groffen, A. J., Sørensen Jakob B., J. B. & Verhage, M. Multiple  $\text{Ca}^{2+}$  sensors in secretion: Teammates, competitors or autocrats? *Trends Neurosci.* 34, 487–497 (2011).
110. Sun, J. et al. A dual- $\text{Ca}^{2+}$ -sensor model for neurotransmitter release in a central synapse. *Nature* 450, 676–82 (2007).
111. Kochubey, O. & Schneggenburger, R. Synaptotagmin Increases the Dynamic Range of Synapses by Driving  $\text{Ca}^{2+}$ -Evoked Release and by Clamping a Near-Linear Remaining  $\text{Ca}^{2+}$  Sensor. *Neuron* 69, 736–748 (2011).
112. Liu, H., Dean, C., Arthur, C. P., Dong, M. & Chapman, E. R. Autapses and networks of hippocampal neurons exhibit distinct synaptic transmission phenotypes in the absence of synaptotagmin I. *J. Neurosci.* 29, 7395–7403 (2009).
113. Broadie, K., Bellen, H. J., DiAntonio, A., Littleton, J. T. & Schwarz, T. L. Absence of synaptotagmin disrupts excitation-secretion coupling during synaptic transmission. *Proc. Natl. Acad. Sci. U. S. A.* 91, 10727–31 (1994).
114. Xu, J., Pang, Z. P., Shin, O. & Südhof, T. C. Synaptotagmin-1 functions as a  $\text{Ca}^{2+}$  sensor for spontaneous release. *Nat. Neurosci.* 12, 759–766 (2009).
115. Chang, S., Trimbuch, T. & Rosenmund, C. Synaptotagmin-1 drives synchronous  $\text{Ca}^{2+}$ -triggered fusion by C2B-

- domain-mediated synaptic-vesicle-membrane attachment. *Nat. Neurosci.* 21, 33–40 (2018).
116. Littleton, J. T., Stern, M., Schuize, K., Perin, M. & S, H. J. B. Mutational Analysis of *Drosophila* Demonstrates Its Essential Role in  $\text{Ca}^{2+}$ -Activated Neurotransmitter synaptotagmin Release. *Cell* 74, 1125–1134 (1993).
  117. Sheng, Z. H., Yokoyama, C. T. & Catterall, W. A. Interaction of the synprint site of N-type  $\text{Ca}^{2+}$  channels with the C2B domain of synaptotagmin I. *Proc. Natl. Acad. Sci. U. S. A.* 94, 5405–10 (1997).
  118. Charvin, N. et al. Direct interaction of the calcium sensor protein synaptotagmin I with a cytoplasmic domain of the  $\alpha 1A$  subunit of the P/Q-type calcium channel. *EMBO J.* 16, 4591–6 (1997).
  119. Seagar, M. et al. Interactions between proteins implicated in exocytosis and voltage-gated calcium channels. *Philos. Trans. R. Soc. Lond. B. Biol. Sci.* 354, 289–97 (1999).
  120. Díez-Azola, R. et al. Doc2 proteins are not required for the increased spontaneous release rate in synaptotagmin-1 deficient neurons. *J. Neurosci.* (2020). doi:10.1523/JNEUROSCI.0309-19.2020
  121. Liu, H. et al. Synaptotagmin 7 functions as a  $\text{Ca}^{2+}$ -sensor for synaptic vesicle replenishment. *Elife* 3, e01524 (2014).
  122. Turecek, J., Jackman, S. L. & Regehr, W. G. Synaptotagmin 7 confers frequency invariance onto specialized depressing synapses. *Nature* 551, 503–506 (2017).
  123. Bai, H. et al. Different states of synaptotagmin regulate evoked versus spontaneous release. *Nat. Commun.* 7, 10971 (2016).
  124. Vasin, A., Volfson, D., Littleton, J. T. & Bykhovskaia, M. Interaction of the Complexin Accessory Helix with Synaptobrevin Regulates Spontaneous Fusion. *Biophys. J.* 111, 1954–1964 (2016).
  125. Xue, M. et al. Distinct domains of complexin I differentially regulate neurotransmitter release. *Nat. Struct. Mol. Biol.* 14, 949–58 (2007).
  126. Lai, Y. et al. Complexin inhibits spontaneous release and synchronizes  $\text{Ca}^{2+}$ -triggered synaptic vesicle fusion by distinct mechanisms. *Elife* 3, e03756 (2014).
  127. Zhou, Q. et al. The primed SNARE-complexin-synaptotagmin complex for neuronal exocytosis. *Nature* 548, 420–425 (2017).
  128. Wierda, K. D. B. & Sorensen, J. B. Innervation by a GABAergic Neuron Depresses Spontaneous Release in Glutamatergic Neurons and Unveils the Clamping Phenotype of Synaptotagmin-1. *J. Neurosci.* 34, 2100–2110 (2014).
  129. Turecek, J. & Regehr, W. G. Neuronal Regulation of Fast Synaptotagmin Isoforms Controls the Relative Contributions of Synchronous and Asynchronous Release. *Neuron* (2019). doi:10.1016/j.neuron.2019.01.013
  130. Geppert, M. et al. Synaptotagmin I: a major  $\text{Ca}^{2+}$  sensor for transmitter release at a central synapse. *Cell* 79, 717–27 (1994).
  131. Sugita, S., Shin, O.-H., Han, W., Lao, Y. & Südhof, T. C. Synaptotagmins form a hierarchy of exocytotic  $\text{Ca}^{2+}$  sensors with distinct  $\text{Ca}^{2+}$  affinities. *EMBO J.* 21, 270–80 (2002).
  132. Brouwer, I. et al. Direct quantitative detection of Doc2b-induced hemifusion in optically trapped membranes. *Nat. Commun.* 6, 8387 (2015).
  133. Sorkin, R. et al. Synaptotagmin-1 and Doc2b Exhibit Distinct Membrane-Remodeling Mechanisms. *Biophys. J.* 118, 643–656 (2020).
  134. Ritzau-Jost, A. et al. Apparent calcium dependence of vesicle recruitment. *J. Physiol.* 596, 4693–4707 (2018).
  135. Wang, L. Y. & Kaczmarek, L. K. High-frequency firing helps replenish the readily releasable pool of synaptic vesicles. *Nature* 394, 384–8 (1998).
  136. Babai, N., Bartoletti, T. M. & Thoreson, W. B. Calcium regulates vesicle replenishment at the cone ribbon synapse. *J. Neurosci.* 30, 15866–77 (2010).
  137. Hvalby, O., Jensen, V., Kao, H.-T. & Walaas, S. I. Synapsin-dependent vesicle recruitment modulated by forskolin, phorbol ester and  $\text{Ca}^{2+}$  in mouse excitatory hippocampal synapses. *Front. Synaptic Neurosci.* 2, 152 (2010).
  138. Lipstein, N. et al. Dynamic control of synaptic vesicle replenishment and short-term plasticity by  $\text{Ca}^{2+}$ -calmodulin-Munc13-1 signaling. *Neuron* 79, 82–96 (2013).
  139. Sakaba, T. & Neher, E. Calmodulin mediates rapid recruitment of fast-releasing synaptic vesicles at a calyx-type synapse. *Neuron* 32, 1119–31 (2001).
  140. Weber, T. et al. SNAREpins: Minimal Machinery for Membrane Fusion. *Cell* 92, 759–772 (1998).
  141. Rizo, J. & Rosenmund, C. Synaptic vesicle fusion. *Nat. Struct. Mol. Biol.* 15, 665–74 (2008).
  142. Wang, Z., Liu, H., Gu, Y. & Chapman, E. R. Reconstituted synaptotagmin I mediates vesicle docking, priming, and fusion. *J. Cell Biol.* 195, 1159–70 (2011).
  143. Zanetti, M. N. et al. Ring-like oligomers of Synaptotagmins and related C2 domain proteins. *Elife* 5, (2016).
  144. Ramakrishnan, S. et al. Synaptotagmin oligomers are necessary and can be sufficient to form a  $\text{Ca}^{2+}$ -sensitive fusion clamp. *FEBS Lett.* 593, 154–162 (2019).
  145. Martens, S. Role of C2 domain proteins during synaptic vesicle exocytosis. *Biochem. Soc. Trans.* 38, 213–216

- (2010).
146. Nikolaus, J., Warner, J. M., O'shaughnessy, B. & Herrmann, A. C2 Domains and Membrane Fusion. *Membr. Fusion* 68, 1–32 (2011).
  147. Zeisel, A. et al. Cell types in the mouse cortex and hippocampus revealed by single-cell RNA-seq. *Science* (80-.). 347, 1138–1142 (2015).
  148. Gokce, O. et al. Cellular Taxonomy of the Mouse Striatum as Revealed by Single-Cell RNA-Seq. *Cell Rep.* 16, 1126–1137 (2016).
  149. Liu, P., Khvotchev, M., Li, Y. C., Chanaday, N. L. & Kavalali, E. T. Copine-6 Binds to SNAREs and Selectively Suppresses Spontaneous Neurotransmission. *J. Neurosci.* 38, 5888–5899 (2018).
  150. Dityatev, A. E., Kozhanov, V. M. & Gapanovich, S. O. Modeling of the quantal release at interneuronal synapses: analysis of permissible values of model moments. *J. Neurosci. Methods* 43, 201–214 (1992).
  151. Stevens, C. F. & Wang, Y. Facilitation and depression at single central synapses. *Neuron* 14, 795–802 (1995).
  152. Zucker, R. S. Minis: Whence and Wherefore? *Neuron* 45, 482–484 (2005).
  153. Smith, S. M. et al. Calcium regulation of spontaneous and asynchronous neurotransmitter release. *Cell Calcium* 52, 226–33 (2012).
  154. Lu, T. & Trussell, L. O. Inhibitory Transmission Mediated by Asynchronous Transmitter Release. *Neuron* 26, 683–694 (2000).
  155. Carter, A. G. & Regehr, W. G. Quantal events shape cerebellar interneuron firing. *Nat. Neurosci.* 5, 1309–18 (2002).
  156. Farrant, M. & Nusser, Z. Variations on an inhibitory theme: phasic and tonic activation of GABA(A) receptors. *Nat. Rev. Neurosci.* 6, 215–29 (2005).
  157. Frank, C. A., Kennedy, M. J., Goold, C. P., Marek, K. W. & Davis, G. W. Mechanisms underlying the rapid induction and sustained expression of synaptic homeostasis. *Neuron* 52, 663–77 (2006).
  158. Turrigiano, G. G., Leslie, K. R., Desai, N. S., Rutherford, L. C. & Nelson, S. B. Activity-dependent scaling of quantal amplitude in neocortical neurons. *Nature* 391, 892–6 (1998).
  159. Ehlers, M. D., Heine, M., Groc, L., Lee, M.-C. & Choquet, D. Diffusional trapping of GluR1 AMPA receptors by input-specific synaptic activity. *Neuron* 54, 447–60 (2007).
  160. Crawford, D. C., Ramirez, D. M. O., Trauterman, B., Monteggia, L. M. & Kavalali, E. T. Selective molecular impairment of spontaneous neurotransmission modulates synaptic efficacy. *Nat. Commun.* 8, 14436 (2017).
  161. Gonzalez-Islas, C., Bülow, P. & Wenner, P. Regulation of synaptic scaling by action potential-independent miniature neurotransmission. *J. Neurosci. Res.* 96, 348–353 (2018).
  162. Murphy, T. et al. Differential regulation of calcium/calmodulin-dependent protein kinase II and p42 MAP kinase activity by synaptic transmission. *J. Neurosci.* 14, 1320–1331 (1994).
  163. Sutton, M. A., Wall, N. R., Aakalu, G. N. & Schuman, E. M. Regulation of dendritic protein synthesis by miniature synaptic events. *Science* 304, 1979–83 (2004).
  164. Andreae, L. C., Fredj, N. Ben & Burrone, J. Independent vesicle pools underlie different modes of release during neuronal development. *J. Neurosci.* 32, 1867–74 (2012).
  165. Desai, N. S., Cudmore, R. H., Nelson, S. B. & Turrigiano, G. G. Critical periods for experience-dependent synaptic scaling in visual cortex. *Nat. Neurosci.* 5, 783–9 (2002).
  166. Young, S. H. & Poo, M. M. Spontaneous release of transmitter from growth cones of embryonic neurones. *Nature* 305, 634–7 (1983).
  167. Andreae, L. C. & Burrone, J. Spontaneous Neurotransmitter Release Shapes Dendritic Arbors via Long-Range Activation of NMDA Receptors. *Cell Rep.* 10, 873–882 (2015).
  168. Sutton, M. A. & Schuman, E. M. Dendritic protein synthesis, synaptic plasticity, and memory. *Cell* 127, 49–58 (2006).
  169. Andreae, L. C. & Burrone, J. The role of spontaneous neurotransmission in synapse and circuit development. *J. Neurosci. Res.* 96, 354–359 (2018).
  170. McKinney, R. A., Capogna, M., Dürr, R., Gähwiler, B. H. & Thompson, S. M. Miniature synaptic events maintain dendritic spines via AMPA receptor activation. *Nat. Neurosci.* 2, 44–9 (1999).
  171. Guarnieri, F. C., de Chevigny, A., Falace, A. & Cardoso, C. Disorders of neurogenesis and cortical development. *Dialogues Clin. Neurosci.* 20, 255–266 (2018).
  172. Parrini, E., Conti, V., Dobyns, W. B. & Guerrini, R. Genetic Basis of Brain Malformations. *Mol. Syndromol.* 7, 220–233 (2016).
  173. Nagode, D. A. et al. Abnormal Development of the Earliest Cortical Circuits in a Mouse Model of Autism Spectrum Disorder. *Cell Rep.* 18, 1100–1108 (2017).
  174. Lewis, D. A. & Sweet, R. A. Schizophrenia from a neural circuitry perspective: advancing toward rational pharmacological therapies. *J. Clin. Invest.* 119, 706–16 (2009).

175. Golovin, R. M. & Broadie, K. Neural Circuits: Reduced Inhibition in Fragile X Syndrome. *Curr. Biol.* 27, R298–R300 (2017).
176. Hu, X., Tang, J., Lan, X. & Mi, X. Increased expression of DOC2A in human and rat temporal lobe epilepsy. *Epilepsy Res.* 151, 78–84 (2019).
177. Glessner, J. T. et al. Strong synaptic transmission impact by copy number variations in schizophrenia. *Proc. Natl. Acad. Sci.* 107, 10584–10589 (2010).



